



Faculty of Science Technology
Department of Electrical Engineering

Master Dissertation

In obtaining of MASTER Degree - ACADEMIC

Domain: Sciences and Technology

Sector: **Automatic**

Speciality: **Automatic and Systems**

TOPIC

Robust control of a wind turbine based on a permanent magnet generator by state feedback linearization.

Presented by:

- Abir Kamel
- Ikram Brakni

Board of Examiners

- | | | |
|---------------------|------|----------------------|
| - Abdalhak Loudjani | MAA | President |
| - Amel Bouchemha | MCA | Supervisor |
| - Sami Kahla | MCA | Co-supervisor |
| - Youcef Soufi | Prof | Examiner |



DEPARTEMENT DE GENIE ELECTRIQUE

MEMOIRE

DE FIN D'ETUDES POUR L'OBTENTION DU DIPLOME DE MASTER EN

Domaine : Sciences et technologie

Filière : Automatique

Spécialité : Automatique et système

THEME

**Commande robuste d'une éolienne basée sur une
génératrice à aimants permanents par linéarisation à
retour d'état.**

Présenté par le binôme :

- Abir Kamel
- Ikram Brakni

Devant le jury :

- Abdalhak Loudjani	MAA	Président
- Amel Bouchemha	MCA	Rapporteur
- Sami Kahla	MCA	Co- rapporteur
- Youcef Soufi	Prof	Examineur

بِسْمِ اللَّهِ الرَّحْمَنِ الرَّحِيمِ



Acknowledgement

First, we thank Almighty Allah for having granted us Health, courage and the means to pursue our studies.

The will, patience and luck to complete this work.

We would like to thank our supervisors Professor **Bouchemha Amel and Doctor Kahla Sami** for supporting us, for your guidance, your advice and your scientific abilities. Your skills were our great support, as well as your availability and especially your kindness which we appreciate very much, for the freedom that you have given us and the responsibilities that you have entrusted to us have contributed greatly to the formation of our personality and our autonomy in our work.

We would also like to thank all **the members of the jury**. We would for the support and attention they gave us throughout the entire throughout the examination.

Finally, we cannot forget all the people at **University of Cheikh El Arbi Tebessi**. We thank them sincerely for having given us this level of study, this level which has our real support and backing during this work and it will continue to do so throughout our along our professional academic path.



DEDICATION

In order to be grateful to those who have supported and encouraged me in this research work, I dedicate this thesis :

To my very dear father for his moral support, and for all the feelings of affection and love which are the pillar of all my efforts.

To my dearest mother.

To all the members of my family, without exception.

And to all those who hold my success dear to their hearts.

I dedicate this thesis to my first relatives:

To my mother who passed away not long ago, I hope that Allah will have His Mercy.

To my mum who was always by my side in good times and bad.

To my brothers and sisters.

I dedicate this thesis to all my teachers throughout my student life.

I also dedicate this thesis to all my friends.

Abir Kamel



DEDICATE

I thank Allah, the Highest, the Almighty, who has bestowed upon me by His grace the spirit and religion, who says in the decisive revelation: "And over every possessor of knowledge".

I dedicate this graduation to the one who taught me to give and to the one whose name I bear with pride. 'Papito'

And to whom her supplication was the secret of my success, and she put me on the path of life and took care of me until I became a great "Mama"

To my brothers and sisters who have had a great impact on many obstacles and difficulties «Randa, Chawki, Amin, Chiheb, Ahmed, Abd al Rahim. Riham»

To the Brakni family

To all my friends, «Khawla, Djihan, Ghada, Najat, Lineb, Omayma, ahlem»

I also dedicate this graduation to my professors in the College of Science and Technology, Department of Electrical Engineering, specializing in automatique and systems

Finally, my sincere thanks to all those who reached out and helped to produce this study to the fullest.

Ikram Brakni



Acronyms and Symbols

Acronyms

DC/AC	Direct current/Alternative current
DC/DC	Direct current / Direct current
FLC	Feedback Linearization Control
INC	Incremental conductance
IPC	Indirect power control
HAWT	Horizontal-axis wind turbines
Lie	Lie derivation
MAS	Asynchronous machine
MPPT	Maximum Power Point Tracking
MSC	Synchronous machine
NC	Nichols Chart
ORB	Optimal relation based
OT	Optimal Torque
PSF	Power signal flow
P&O	Perturbation and Observation
PI	Proportional Integrator
PMSG	Permanent Magnet Synchronous Generator
TSR	Tip Speed Ratio
VAWT	Vertical-axis wind turbine
WECS	Wind Energy Conversion System

Symbols

C_p	Power coefficient
C_{pmax}	Limite de Betz du coefficient de puissance
dEc	Kinetic energy of the wind (J)
G	multiplier gain
J_h	Total shaft moment inertia
L_d, L_L, L_q	Stator inductance.
P	Number of poles.
P_{aer}	Aerodynamic power [W]
P_m	Mechanical power [W]
R	Wind turbine rotor radius[m].
R_{ch}	Charge resistance
R_s	Stator resistance.
$u(t)$	Control input
$V(t)$	Wind velocity [m/s]
β	Rotor blade pitch angle [rad.]

λ	Tip-speed-ratio (TSR)
λ_{opt}	Optimal tip-speed-ratio
Γ_A	Aerodynamic torque
Γ_T	Wind turbine torque
Γ_{em}	electromagnetic torque
Ω_t	Angular velocity [rad/s].
Ω_{tn}	Nominal angular velocity [rad/s].
Ω_h	Generator shaft speed [rad/s]
Φ_m	Magnet flux
ρ	Density of air [kg/m ³]

List of figures

Fig.I.1	Wind energy conversion Principle diagram.....	4
Fig.I.2	Different size and power of wind turbines over the years.....	5
Fig.I.3	Wind turbine types.....	5
Fig.I.4	Vertical axis wind types.....	6
Fig.I.5	Horizontal axis wind turbine designs.....	7
Fig.I.6	Wind turbine configurations.....	7
Fig.I.7	Horizontal axis wind turbine parts.....	8
Fig.I.8	Main internal components of a wind turbine nacelle.....	8
Fig.I.9	a) Wind power operating region; b) typical variable and fixed wind speed power curves.....	10
Fig.I.10	Wind column kinetic energy.....	11
Fig.I.11	Current tube around a wind turbine.....	11
Fig.I.12	Aerodynamic power coefficient as a function of (TSR).....	12
Fig. I.13	Asynchronous machine connected directly to the grid.....	14
Fig.I.14:	Wind energy system based on the permanent magnet synchronous machine.....	15
Fig.II.1	Block diagram of Permanent magnet synchronous generators in WECS systems; (a) Complete and (b) Equivalent diagram.....	17
Fig.II.2	Mechanical system of the turbine.....	20
Fig.II.3	Simplified turbine model.....	21
Fig.II.4	Diagram of the WECS system based on PMSG.....	21
Fig.II.5	Block diagram of turbine model.....	22
Fig.II.6	Transition from a three-phase system (permanent magnet).....	22
Fig.II.7	Equivalent Electrical model in reference frame (d, q).....	24
Fig.II.8	Feedback linearization control of PMSG-based WECS.....	26.
Fig.II.9	MPPT with the optimal specific speed (TSR).....	27
Fig.II.10	Diagram of PSF MPPT algorithm.....	28
Fig.II.11	MPPT based Optimal torque control (OTC).....	28
Fig.II.12	State-feedback control.....	31
Fig.II.13	Feedback linearization control of PMSG-based WECS.....	32
Fig.II.14	TSR control based on PI controller.....	32
Fig.II.15	Mathematical calculation of (k_u) and (T_u).....	33
Fig.III.1	WECS Block Diagram without MPPT Control.....	36
Fig.III.2	Power Coefficient C_p	37

Fig.III.3	Tip speed ratio λ	37
Fig.III.4	Mechanical power P_m	38
Fig.III.5	MPPT control simulation using a PI controller diagram block.....	38
Fig.III.6	MPPT control simulation via Feedback linearization controller diagram block....	39
Fig.III.7	Wind speed profile with low disturbance.....	40
Fig.III.8	Power coefficient $C_p(t)$ for a FL controller versus a PI controller.....	40
Fig.III.9	Specific speed $\lambda(t)$ for a FL controller versus a PI controller.....	41
Fig.III.10	Generator speed for an FL controller versus a PI controller.....	41
Fig.III.11	Turbine speed for a FL controller versus a PI controller.....	42
Fig.III.12	Electromagnetic torque for a FL controller versus a PI controller.....	43
Fig.III.13	Aerodynamic torque for a FL controller versus a PI controller.....	43
Fig.III.14	Electrical power for a FL controller versus a PI controller.....	44
Fig.III.15	Mechanical power for a FL controller versus a PI controller.....	44
Fig.III.16	Wind speed profile with high disturbance.....	45
Fig.III.17	Power coefficient $C_p(t)$ for a FL controller versus a PI controller.....	46
Fig.III.18	Tip speed ratio $\lambda(t)$ for a FL controller versus a PI controller.....	47
Fig.III.19	Generator speed for a FL controller versus a PI controller.....	47
Fig.III.20	Turbine speed for a FL controller versus a PI controller.....	48
Fig.III.21	Electromagnetic torque for a FL controller versus a PI controller.....	48
Fig.III.22	Aerodynamic torque for a FL controller versus a PI controller.....	49
Fig.III.23	Electrical power for a FL controller versus a PI controller.....	49
Fig.III.24	Mechanical power for a FL controller versus a PI controller.....	49

List of tables

Table I.1	Classification of wind turbines.....	4
Table III.1	Parameters of the low-power (3-kW) WECS equipped with PMSG.....	32

Abstract

Wind energy conversion systems (WECSs) are considered generators, environmentally friendly, and fully suitable energy sources to replace fossil energy sources. The presented work is dedicated to the study and modelling of linear and robust control strategies for the maximum power extraction of an autonomous wind energy conversion system based on a permanent magnet synchronous generator (PSMG) under different wind speeds and which is of small power intended for the electrification of isolated sites. Mathematical models of each part of the chain are developed and simulated using Matlab/Simulink. In addition, the maximum power point tracking (MPPT) of the WECS based on PMSG is controlled to ensure optimum operation. For this reason, we used a robust control technique based on feedback linearization control, where the system's non-linearity problems and parametric uncertainty are considered, ensuring robustness of the control to potential disturbances and enabling maximum power to be extracted under stochastic wind conditions. The performance of the designed controller was compared with the conventional PI controller for low turbulence stochastic wind speed and high turbulence stochastic wind speed.

Keywords: Wind energy conversion system (WECS), MPPT, PMSG, classical PI, feedback linearization control.

ملخص

تعتبر أنظمة تحويل طاقة الرياح (WECSs) مولدات صديقة للبيئة ومصادر طاقة مناسبة تمامًا لتحل محل مصادر الطاقة الأحفورية. العمل المقدم مكرس لدراسة ونمذجة استراتيجيات التحكم الخطية والقوية لاستخراج الطاقة القصوى لنظام تحويل طاقة الرياح المستقل على أساس مولد مترامن مغناطيسي دائم (PSMG) تحت سرعات رياح مختلفة والتي تكون ذات طاقة صغيرة مخصصة لـ كهربية المواقع المعزولة. تم تطوير النماذج الرياضية لكل جزء من السلسلة ومحاكاتها باستخدام Matlab / Simulink. بالإضافة إلى ذلك، يتم التحكم في الحد الأقصى لتتبع نقطة الطاقة (MPPT) الخاص بـ WECS استنادًا إلى PMSG لضمان التشغيل الأمثل. لهذا السبب، استخدمنا تقنية تحكم قوية تعتمد على التحكم في التغذية الراجعة الخطية، حيث يتم أخذ مشاكل النظام غير الخطية وعدم اليقين المعياري في الاعتبار، مما يضمن متانة التحكم في الاضطرابات المحتملة وتمكين استخراج أقصى طاقة في ظل ظروف الرياح العشوائية. تمت مقارنة أداء وحدة التحكم المصممة مع وحدة التحكم التقليدية PI لسرعة الرياح العشوائية المنخفضة والاضطراب وسرعة الرياح العشوائية عالية الاضطراب

الكلمات المفتاحية: سلسلة تحويل توربينات الرياح، مولد التزامن المغناطيسي الدائم، التحكم الكلاسيكي PI، والتحكم في التغذية المرتدة، التحكم في خطية التغذية الراجعة.

Résumé

Les systèmes de conversion de l'énergie éolienne (SCEE) sont considérés comme des générateurs respectueux de l'environnement, et comme des sources d'énergie parfaitement adaptées pour remplacer les sources d'énergie fossiles. Le travail présenté est consacré à l'étude et à la modélisation de stratégies de contrôle linéaires et robustes pour l'extraction de puissance maximale d'un système autonome de conversion d'énergie éolienne basé sur un générateur synchrone à aimant permanent (GSAP) sous différentes vitesses de vent et qui est de petite puissance destinée à l'électrification de sites isolés. Les modèles mathématiques de chaque partie de la chaîne sont développés et simulés à l'aide de Matlab/Simulink. En outre, le suivi du point de puissance maximale (MPPT) du SCEE basé sur le GSAP est contrôlé pour assurer un fonctionnement optimal. Pour cette raison, nous avons utilisé une technique de contrôle robuste basée sur le contrôle de linéarisation par rétroaction, où les problèmes de non-linéarité du système et l'incertitude paramétrique sont pris en compte, assurant la robustesse du contrôle aux perturbations potentielles et permettant l'extraction d'une puissance maximale dans des conditions de vent stochastiques. Les performances du régulateur conçu ont été comparées à celles du régulateur PI conventionnel pour une vitesse de vent stochastique à faible turbulence et une vitesse de vent stochastique à forte turbulence.

Mots clés: Système de conversion éolienne (SCEE), puissance maximale, GSAP, PI classique, linéarisation en retour d'état.

Table of contents

List of Acronyms and Symbols.....	I
List of figures.....	VIII
List of tables.....	VIII
Abstract.....	VIII
General Introduction.....	1

Chapter I Wind Power Generation Systems

I. Introduction	3
II. Theoretical concepts about wind energy.....	3
II.1. Wind Energy Conversion System.....	4
II.2. Classification of wind turbines.....	4
II.2.1. Wind generators according to the power range.....	5
II.2.2. Types of Wind Turbine Rotors.....	5
II.2.2.1. Vertical Axis Wind Turbines.....	6
II.2.2.2. Horizontal Axis Wind Turbines	7
III. Principle elements of Horizontal Axis Wind turbines	9
IV. Aerodynamic power control mechanism of WECS.....	10
IV.1. Wind Turbine Operating zone (Power Cur.....	10
IV.2. Conversion of kinetic energy of the wind into mechanical energy.....	11
IV.2.1 Power Coefficient (Betz's Law).....	13
IV.2.2 The specific or normalized speed (Tip-Speed-Ratio).....	13
IV.2.3 Torque coefficient.....	13
V. Ways of exploiting wind energy.....	14
V.1 Fixed speed turbine.....	14
V.2.Variable Speed System.....	15
VI. Conclusion.....	15

Chapter II Modeling and Feedback Linearization control of WECS in autonomous mode

I. Introduction.....	16
II. Model of the Wind Energy Conversion System.....	16
II.1. Aerodynamic Part.....	16
II.1.1 Model of the wind.....	17
II.1.2. Aerodynamic model of the wind turbine.....	18
II.2. Modeling of mechanical part.....	19
II.2.1 Model of the multiplier.....	21
II.2.2. Modeling of the permanent magnet synchronous generator.....	22
III. MPPT Controller Based on Feedback Linearization Method.....	25
III.1. Maximum Power Point Tracking Algorithms.....	25
III.1.1 MPPT algorithms based on IPC.....	26
IV. PSMG-WECS Controller Design Based on Feedback Linearization.....	29
V. MPPT-TSR control based on a PI controller.....	32
VI. Conclusion.....	33

Chapter 03 Results and interpretation

I. Introduction.....	
II. WECS simulation results without control MPPT.....	35
III. WECS simulation results with control MPPT.....	36

III.1 Comparative study (PI controller and FL controller).....	38
III.1.1. Low-turbulence wind speed (DSP noise=0.001).....	39
III.1.2. High-turbulence Wind speed (DSP noise= 0.01).....	39
	45
IV. Conclusion.....	50
General conclusion.....	51
References.....	52



General

Introduction



General introduction

Global demand for electrical energy is increasing steadily, especially with the advent of new technologies for industrial, electronics and computer equipment environmental pollution and the greenhouse effect are posing global economic problems and crises. Various solutions have been proposed and considered. After the oil crisis, some countries took the lead in going nuclear, while others made massive use of renewable energies, particularly wind power [1-40]. Countries are becoming increasingly interested in producing electricity from wind power in order to produce clean, sustainable energy, and the advanced state of research in the field of wind power shows a desire to develop ever more powerful wind turbines capable of capturing the power available in the wind as effectively as possible [1-40].

The random nature of the wind is the key to determining the power output of WECS. Nevertheless, there are solutions that can be used to improve power output, such as adjusting turbine blade profiles, locating installation sites, improving generators, tracking power output, etc [1-40]. The Maximum Power Point Tracking (MPPT) algorithms for WECS are optimal, and the power output of WECS is optimized. Maximum Power Point Tracking (MPPT) algorithms for WECS are optimal and the output power of the wind turbine is f and the most efficient because they are flexible in controlling different variable wind speeds and suitable for all types of WECS. Nevertheless, Maximum Power Point Tracking (MPPT) algorithms for WECS are optimal and the most efficient because they are flexible in controlling different variable wind speeds and are suitable for all types of WECS [1-40].

In the wind power industry, wind turbines installed worldwide are currently based on either fixed-speed or variable-speed turbines. Variable-speed wind turbines were introduced to provide solutions to the problems of fixed-speed operation. Among the various types of electric machine, we find the Permanent Magnet Synchronous Generator (PMSG), which is characterized by high torque density, very low inertia and low inductance. All these features give the machine high performance, efficiency and controllability.

The main problem with wind power systems is the major discrepancy between the irregular nature of the primary source (wind speed is a random, highly non-stationary process with turbulence and extreme variations) and the extremely demanding regulation requirements on power quality [4]. Various robust control structures dealing with the design of different types of control schemes for PMSG-based variable speed wind systems can be found in the literature [11]:

Optimum Tip Speed Ratio (TSR) control, sliding mode control, power signal feed-back (PSF), sliding mode control, and intelligent control. One approach to designing a robust controller can be based on the Feedback Linearization Control (FLC) because the proposed power wind system (PMSG-WECS) is considered highly nonlinear systems [7-11,20-40]. This method is widely used in the design of robust controllers for non-linear systems with uncertainty. The system is globally linearized based the feedback linearization method, and the maximum power point tracking control law is obtained. The objective of this work is to study and design a robust TSR control strategy based on FLC technique to extract the maximum power from a PMSG-WECS system under a stochastic wind speed.

II. Dissertation Organization

The main purpose of our work is to model and control a small power (3KW) wind turbine conversion system. It will be organized into three chapters.

- In the first chapter, we dealt with theoretical concepts on the wind turbine system, defining the process of converting wind energy into electrical energy, the types of wind turbines and electrical machines used with the WECS. The advantages of using the permanent magnet synchronous machine in the wind energy conversion chain.

- In second chapter, we devolve into the modelling and simulation aspects of a wind energy conversion system (WECS). We focus on a specific type of WECS, namely a wind turbine based on permanent magnet synchronous generator (PMSG). we explain the fundamental principles of PMSG operation and its suitability for wind energy applications. Then the mathematical model of a PMSG-based wind energy conversion power system is studied and expressed. Finally, we present the design of an input-state feedback linearization controller for the wind energy conversion system and TSR based on PI controller.

- In the third chapter, we present the simulation results obtained with a detailed interpretation of the performance of the low-power wind energy conversion system (3KW) by PI and feedback linearization controllers in three wind speed cases (no disturbance, low disturbance, and high disturbance).

Finally, we will end this master dissertation with a general conclusion encompassing the work and research prospects for future work.



CHAPTER I

Wind Power Generation Systems



I Introduction

In the recent years there has been an increasing awareness about the climate change (global warming) and the harmful effects of carbon emission [3-25]. This created a higher demand for clean and sustainable energy source like: wind, solar, biomass, tidal etc. In this context, wind is a particularly attractive option. Wind energy is a renewable energy source characterized by the lowest cost of electricity production and the largest resource available [1-25]. Electric energy is generated from wind using a wind turbine and an electric generator. The generated energy can be used either for standalone loads or fed into the power grid through an appropriate power electronic converter. The wind energy has experienced the biggest growth in the past few years. This is because wind energy is a pollution-free resource, has an unlimited potential. Wind power is capable of supplying hundreds of megawatts of power, but the main challenge associated with wind energy conversion is the wasted potential wind power due to changing wind conditions. With each change in wind velocity, the system must be corresponding adjusted to its optimum operating point to allow maximum power transfer. Wind energy systems are either fixed-speed or variable-speed wind turbine systems [1-25].

The purpose of this chapter is to present some of the key concepts related to wind energy conversion systems (WECS). We will present the standards related to the definition of a wind turbine, the electrical machines used and the types of wind turbines used in WECS in general. The last part is dedicated to the description of the wind turbine, its components, the different types and the operating strategies (fixed speed, variable speed).

II Theoretical concepts about wind energy

II.1. Wind Energy Conversion System

The wind energy conversion system (WECS) contains wind turbines and converter converters. Using wind turbines to extract the wind's mechanical energy, the generators convert it into electrical energy, and the converter system is in charge of transferring the generated energy to the power network or a battery bank [6]. The wind turbine converts part of the kinetic energy of the wind into rotating mechanical energy. This energy is transmitted through a drive system, usually consisting of a speed multiplier, an electric generator to produce electricity (see Fig.I.1).

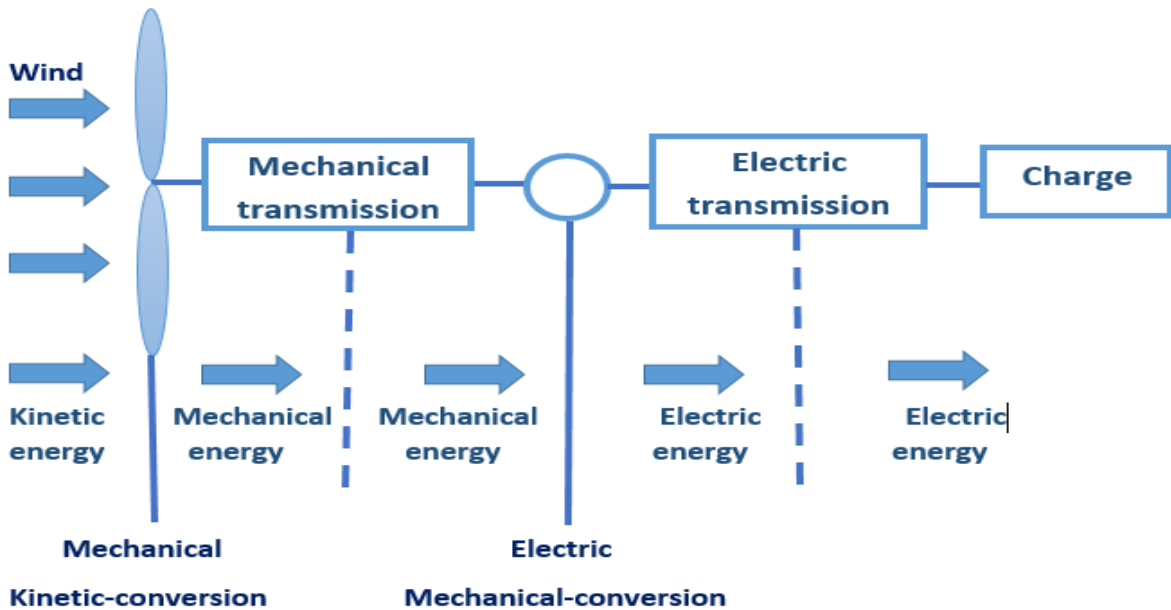


Fig.I.1: Principle diagram of wind energy conversion

II.2. Classification of wind turbines

Wind turbines are classified according to several factors, namely: mode of operation, location 'Offshore' (placed in the sea) or 'Onshore' (placed on the land), and power ranges [7]. The wind turbine consists of two types based on the axis in which the turbine rotates. Turbine which rotates around a horizontal axis (HAWT) is more common than other the type of turbine which rotates around a vertical axis (VAWT) [8].

II.2.1 Wind generators according to the power ranges

Depending on their power, wind turbines can be divided into three categories rated output power, so there are Small wind turbines, medium and high wind turbines Power. The following table summarizes the three categories of wind turbines according to the power they deliver and the diameter of their blade:

Scale	Blade diameters	Power value
Low power	< 12 m	< 40 KW
Medium power	12 to 45 m	40 KW to 1 MW
High power	> 46 m	> 1 MW

Table I.1: Wind turbines classification [9].

Fig (I.2) shows the increase in the average size of wind turbines commercial with time.

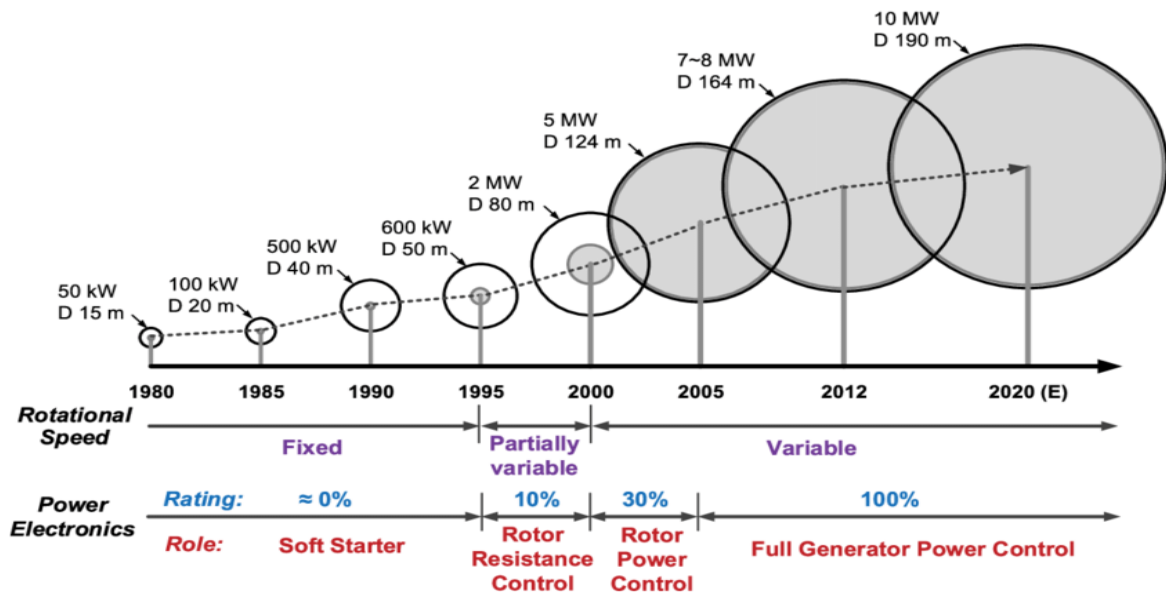


Fig.I.2: Different size and power of wind turbines over the years [10]

II.2.2. Types of Wind Turbine Rotors

Wind turbines are classified according to the geometric arrangement of their shaft on which is mounted the propeller in two types: DARRIEUS vertical axis wind turbines, SAVONIUS mainly and with horizontal axis bipales, tripales and multi-blades [11] (see Fig I.3).

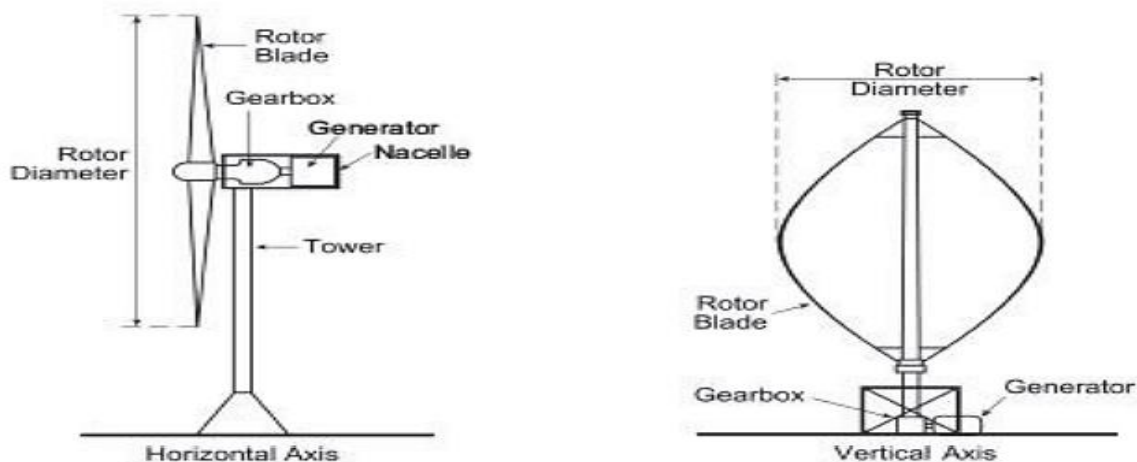


Fig.I.3: Wind turbine types.[9]

II.2.2.1. Axis Wind Turbine (VAWT)

There are two main types of VAWTs, the Savonius and the Darrieus. The Darrieus uses blades similar to those used on HAWTs, while the Savonius operates like a water wheel using drag

forces [13]. The blades rotate around a vertical axis, the turbine is in an optimal position to use this wind. They are the first wind turbines to be used in energy conversion principle of operation is that it rotates around an axis that is perpendicular to the wind direction and vertical to the ground. This type of turbine can receive wind from any direction [14]. In addition, the controls, generator and multiplier are located at ground level, making maintenance easy. There are mainly three types of VAWT (see Fig. I.4)

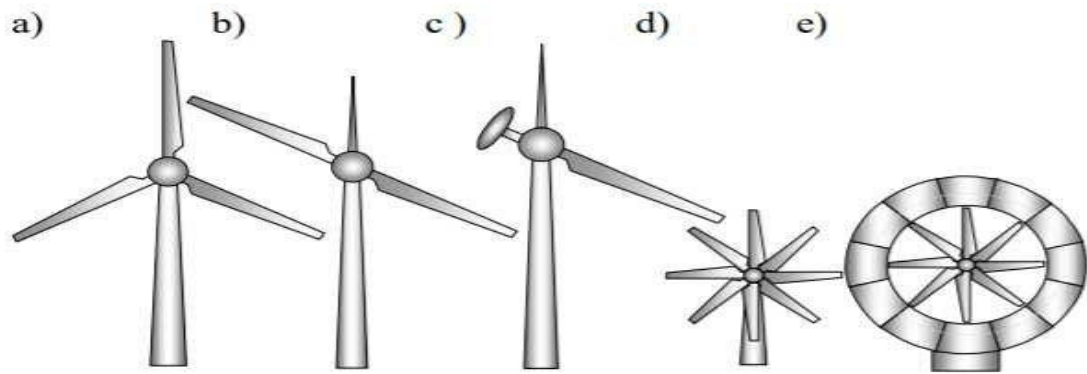


Fig.I.4: Vertical axis wind turbines. [9]

II.2.2.2 Horizontal Axis Wind Turbine (HAWT)

They are the most popular and widely used in high-powered wind farms. The electrical generator and the main rotor shaft are generally placed at the top of a tower for a HAWT [16]. They produce more energy and are less exposed to mechanical stress than vertical axis turbines. The HAWT has a design which is required that should be faced into the wind to obtain maximum power, this process is called yawing [17]. They consist of one or more blades. Due to the trade-off between cost, power coefficient, and rotation speed that characterize three-bladed wind turbines, they are currently the most widely used [18].

In general, the turbine is connected to the shaft of the generator through a gearbox which moves the slow rotation of the blades into a faster rotation that is more suitable to drive an electrical generator [19].



a) three-bladed b) two-bladed c) single-bladed d) multi-bladed e) multi-bladed with

Fig.I.5: Horizontal axis wind turbines Design. [15]

There are two types of horizontal axis wind turbine configurations (see Fig I.6):

- **Upwind rotor:** The wind blows across the front of the blades towards the nacelle. The blades are rigid, and the rotor is steered in the direction of the wind by a device.
- **Downwind rotor:** The wind blows on the back of the blades from the nacelle. The rotor is flexible, self-steering.

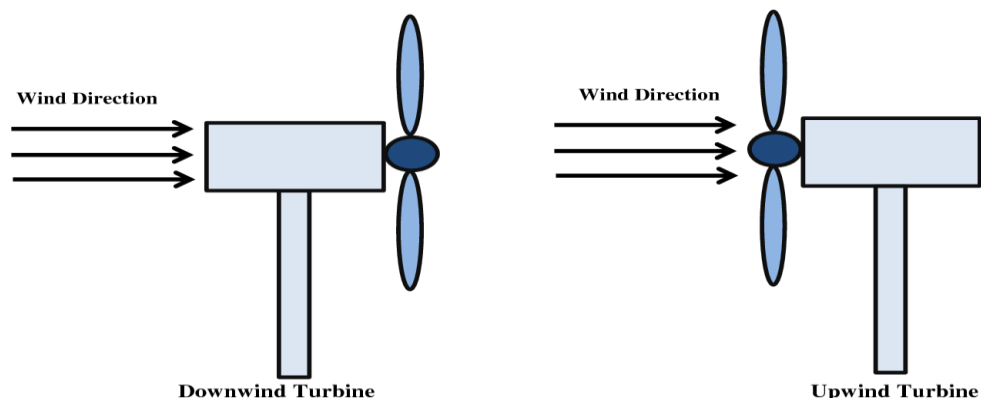


Fig.I.6: Downwind and Upwind rotors.

III. Principle elements of Horizontal Axis Wind turbines

The HAWT consists generally of three blades, supported by a hub forming the rotor and installed at the top of a vertical mast. This assembly is attached to a nacelle housing a generator. An electric motor steers the rotor so that it always faces into the wind. As shown in the above figure, the HAWT consist of several mechanical parts. Some of the parts work to generate the electric power and some parts for protecting the turbine [20].

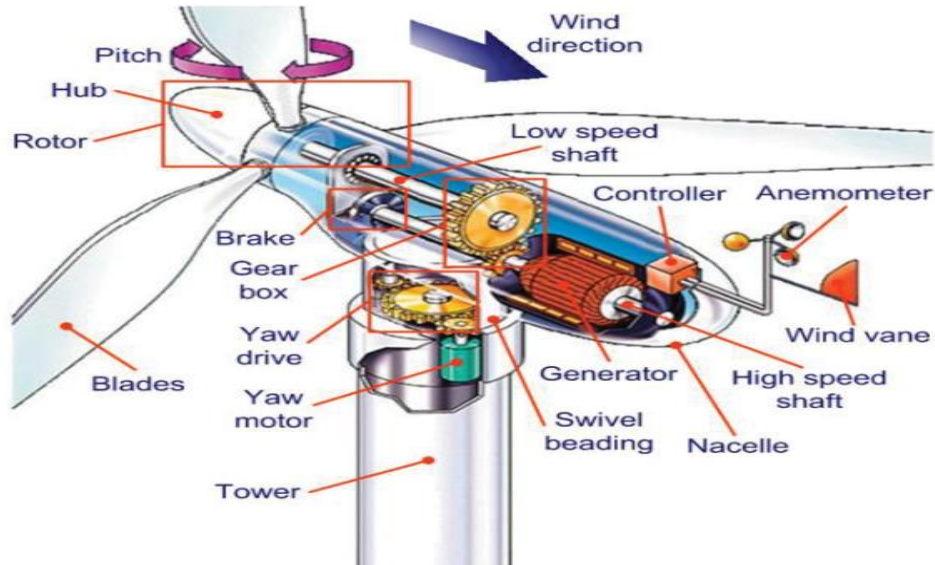


Fig.I.7: Horizontal axis wind turbine parts. [21]

- **Tower (mats)**

Generally a steel tube, or possibly a wire mesh, supports all the equipment used to generate electricity. Its role is to support the rotor and nacelle assembly to prevent the blades from touching the ground and to place the rotor at a sufficient height, to take the rotor as far as possible out of the wind gradient that exists close to the ground, thus improving energy capture.

- **Nacelle**

A housing which contains all the components which is essential to operate the turbine efficiently is called a nacelle. It is fitted at the top of a tower and includes the gear box, low- and high-speed shafts, generator, controller, and brakes. A wind speed anemometer and a wind vane are mounted on the nacelle (see figure above).

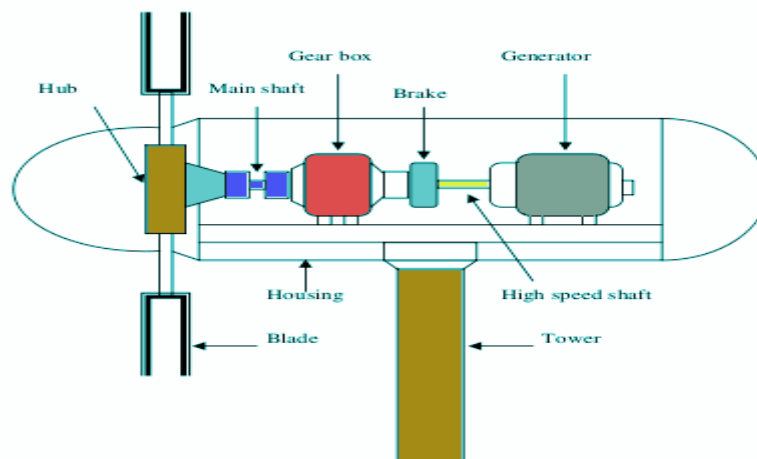


Figure I.8: Main internal components of a wind turbine nacelle [22].

- **Rotor**

The hub and the blades together compose the rotor. The rotor is the rotating part of a wind turbine, capturing and transforming the wind's energy into mechanical energy. The blade of a wind turbine is in fact the real collector of the energy present in the wind, whose number classically varies from 1 to 3; the use of three-bladed rotors is predominant in all medium and high-power machines (> 30 kW). Wind turbine power is proportional to the square of the rotor diameter. There are two types of rotor: fixed-speed and variable-speed [23].

- **Blades**

Wind turbine blades are used to extract the kinetic energy of wind and convert to mechanical energy. These blades are made up of fiber glass-reinforced polyester or wood-epoxy. Wind turbines have one or two or three or multiple blades based up on the construction. Most of the HAWT have three blades [23].

- **Hub**

The hub is the component holds the transmits motion and the rotor together to nacelle and it transmits the loads that which are generated by the blades, most of the hubs are made of steel either cast or welded and there are three main types of them that have been applied in HAWTs: Rigid Hub, Teetering Hub et Hinged Hub [23].

- **Gearbox**

The Gearbox is used in wind energy systems to change low speed high torque power coming from a rotor blade to high speed low torque power which is used for generator. It is connected in between main shaft and generator shaft to increase rotational speeds from about 30 to 60 rotations per minute (rpm) to about 1000 to 1800 rpm [23]. Gearboxes used for wind turbine are made from superior quality aluminium alloys, stainless steel, cast iron etc.

- **Generator**

This alternator converts mechanical energy into electrical energy. The simplest and most robust generators are induction generators. The output rotational mechanical energy of the gear box is connected to the generator through generator shaft. It works on the principle of 'Faraday's law of electromagnetic induction". It converts mechanical energy into electrical energy [23].

IV. Aerodynamic power control mechanism of WECS

IV.1. Wind Turbine Operating zone (Power Curve)

It is important to understand the relationship between power and wind speed to determine the required control type, optimization, or limitation. The Wind speed power characteristic has four zones [28]:

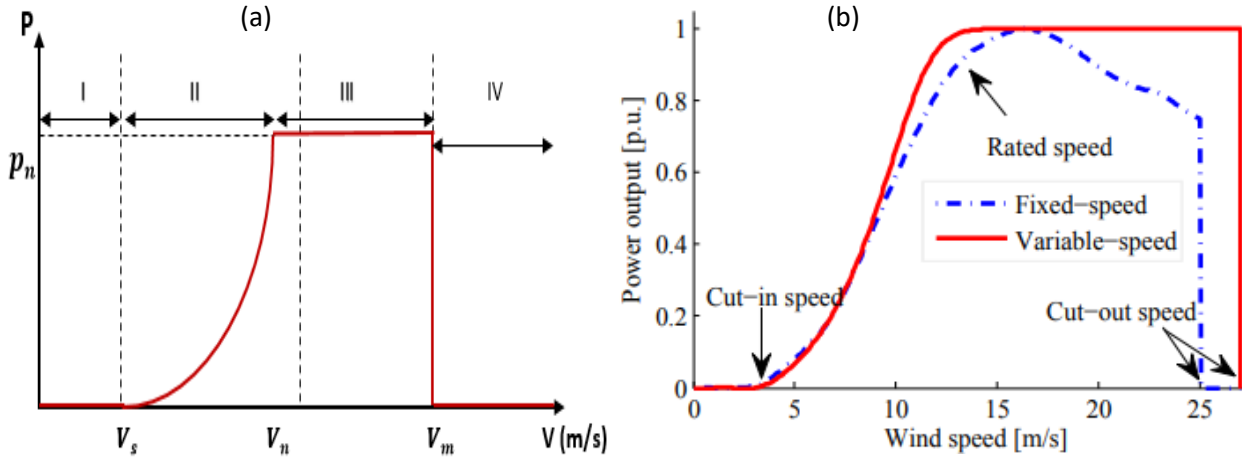


Fig.I.9: a) Wind power operating region; b) typical variable and fixed wind speed power curves [24]

- ✚ **Zone I:** where $P_t = 0$ (the turbine does not provide power).
- ✚ **Zone II:** The wind speed is within the domain $[V_s, V_n]$ corresponds to wind energy conversion. The zone where it is possible to optimize using MPPT system.
- ✚ **Zone III:** The power developed by wind turbine is limited to the nominal power P_m .
- ✚ **Zone IV:** where the safety system stops the rotation and the transfer of energy.

Recall that controlling the pitch of the blade and speed of the generator are the most effective methods to adjust output power. The following control strategies use pitch and generator speed control to manage turbine functionality throughout the power curve: fixed-speed fixed-pitch, fixed-speed variable-pitch, variable-speed fixed-pitch, and variable-speed variable-pitch. Figure Fig. I.8 (b) shows the power curves for variable and fixed wind speed power [24]

IV.2. Conversion of kinetic energy of the wind into mechanical energy

The kinetic energy contained in the wind is transformed in part into mechanical energy by the turbine blades, then into electrical energy via a generator. The kinetic energy of a column of air of length dx of density ρ section S animated by a speed V is written (see Fig.I.6) [25]:

$$dEc = \frac{1}{2} \cdot \rho \cdot A \cdot dx \cdot v^2 \quad (I.1)$$

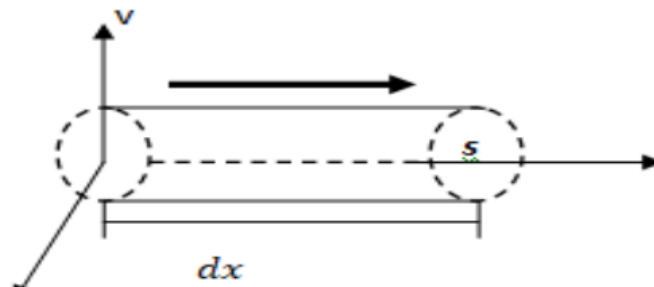


Fig.I.10: Kinetic energy of a wind column.

IV.2.1 Power Coefficient (Betz's Law) [26]

The horizontal axis wind turbine system shown on which the wind speed v_1 upstream of the wind generator and the wind speed v_2 downstream of the generator.

$$C_p = \frac{P_m}{P_t} = \frac{\left(1 + \frac{v_2}{v_1}\right)\left(1 + \frac{v_2^2}{v_1^2}\right)}{2} \tag{I.2}$$

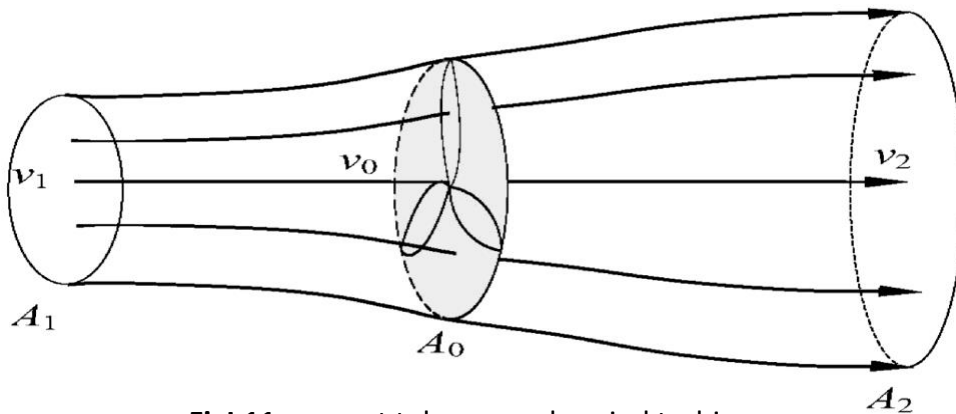


Fig.11: current tube around a wind turbine

The coefficient of power of a wind turbine basically signifies the conversion efficiency of the wind energy of the wind into mechanical energy, which in turn is used to drive the generators. The theorem of the German physicist Betz shows that the maximum energy recoverable in the wind by the rotor is equal to $16 / 27$, or 59.3% of the total energy of the of the total wind energy. In reality, this limit is never reached, and each wind turbine is defined by its own power coefficient expressed as a function of **normalized speed (Tip-Speed-Ratio)** λ . The following figure shows the typical characteristics of the aerodynamic power coefficient C_p for different rotor types. The power coefficient represents the ratio between the power of the rotor and the power available in the wind [25].

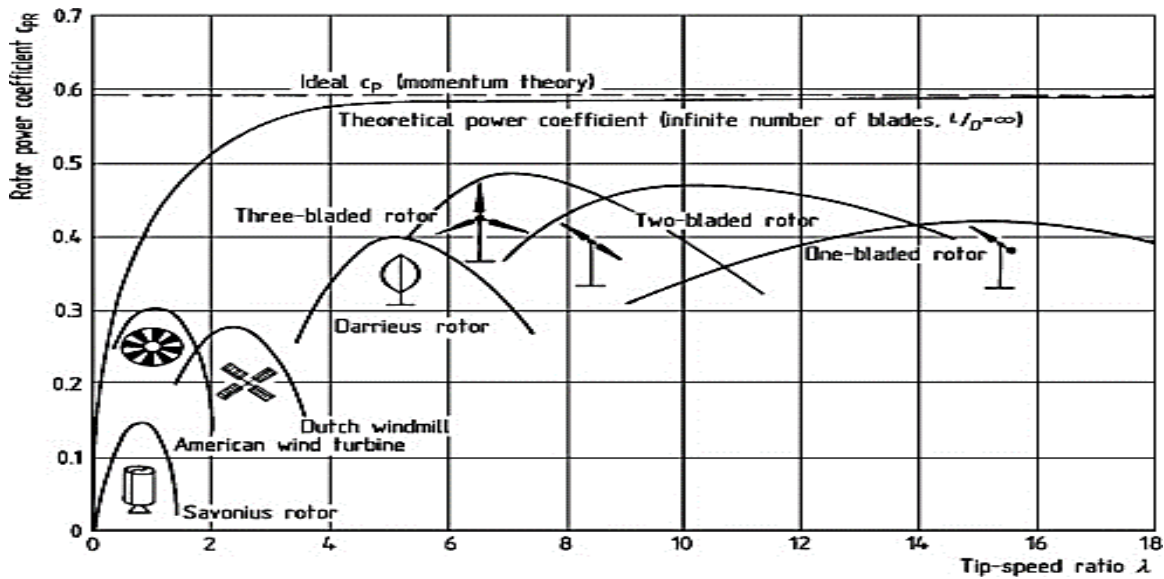


Fig.I.12: Aerodynamic power coefficient as a function of λ [25]

The maximum efficiency of the turbine is therefore [25]:

$$\eta = \frac{16}{27} C_{pmax} \tag{I.3}$$

C_{pmax} :The maximum value of the power coefficient C_p . This value is associated with a nominal specific speed λ_{opt} for which the turbine has been sized according to a nominal wind speed and a nominal rotational speed.

The mass of moving air passing through this tube in a second is given by the product of air density, surface area and mean velocity [27]:

$$m_0 = \frac{\rho \cdot A(v_1 + v_2)}{2} \tag{I.4}$$

With ρ : Air density under normal temperature and pressure conditions (Approximately 1.25kg/m^3 at atmospheric pressure at 15C°) and A : Circular area swept by the turbine.

The actual power extracted by the rotor blades is the difference between the upstream and downstream wind powers [28]. The expression of the aerodynamic power becomes:

$$P_m = m_0 \frac{(v_1^2 - v_2^2)}{2} \tag{I.5}$$

Either by replacing m_0 by its expression in (I.5), we obtain:

$$P_m = \rho \cdot A \frac{(v_1 + v_2)(v_1^2 - v_2^2)}{4} \tag{I.6}$$

A theoretically undisturbed wind would cross this same surface A without any reduction in speed v_1 ; the corresponding power would then be: $P_{m_t} = \rho A \frac{v_1^3}{2}$

IV.2.2 The specific or normalized speed (Tip-Speed-Ratio)

The specific or normalized λ is defined speed as the ratio of the linear speed at the tip of the turbine $\Omega_t \times R_t$ blades on the instantaneous wind speed V and given by the following expression [28]:

$$\lambda = \frac{\Omega_t \times R_t}{V} \quad (I.7)$$

With R_t = Blades radius (m); V = Wind velocity (m/s) and Ω_t : Angular velocity (rad/s).

IV.2.3 Torque coefficient

The torque coefficient C_T is quite close to the power coefficient C_p . It is very useful to estimate the value of the torques for different operating points, in particular at speed Ω_t zero, which corresponds to a value of C_p zero for a value of C_T not zero. By combining equations, the mechanical power P_m available on the shaft of a wind generator can be expressed by [29]:

$$P_m = \frac{1}{2} C_p(\lambda) \rho \pi R^2 V^3 \quad (I.8)$$

Hence the expression of the torque is:

$$\Gamma_t = \frac{P_m}{\Omega_t} = \frac{R_t P_m}{\lambda V} = \frac{C_p}{\lambda} \frac{1}{2} \rho \pi R_t^3 V^2 \quad (I.9)$$

The value of the torque coefficient is determined by the following formula:

$$C_r = \frac{C_p}{\lambda} = \frac{\Gamma_t}{\frac{1}{2} \rho \pi R_t V^2} \quad (I.10)$$

The expression of the mechanical power available on the generator shaft can be expressed by:

$$P_m = \frac{1}{2} C_p \left(\frac{\Omega_t R}{GV_1} \right) \rho R_t V^3 \quad (I.11)$$

V. Wind turbine Configurations and topologies

Numerous electrical machines can be used as generators for wind turbines. These include asynchronous machines, synchronous generators and DC motors. In the wind turbine industry, synchronous and asynchronous generators are the most widely used. Depending on the type of operation, the type of generator and the environment in which the wind turbine is installed, there are several configurations. The most common of which are fixed speed and variable speed [30].

V.1 Fixed speed turbine

Fixed speed wind turbines were the first to be developed. In this technology, the generator is directly coupled to the grid via a transformer. Its mechanical speed is then imposed by the frequency of the grid and the number of pole pairs in the generator. The fixed speed configuration can be represented in a simplified way by the diagram figure (I. 12). The wind energy conversion chain consists of the turbine, the speed the turbine, the speed multiplier and the generator [30]. The fixed mechanical speed is imposed by the grid frequency and the number of pole pairs. The power control for this configuration takes place at turbine level, either by aerodynamic stall, or by variable blade pitch to approximate synchronous operation and it is equipped with a speed multiplier to adapt to the speed of the turbine and generator.

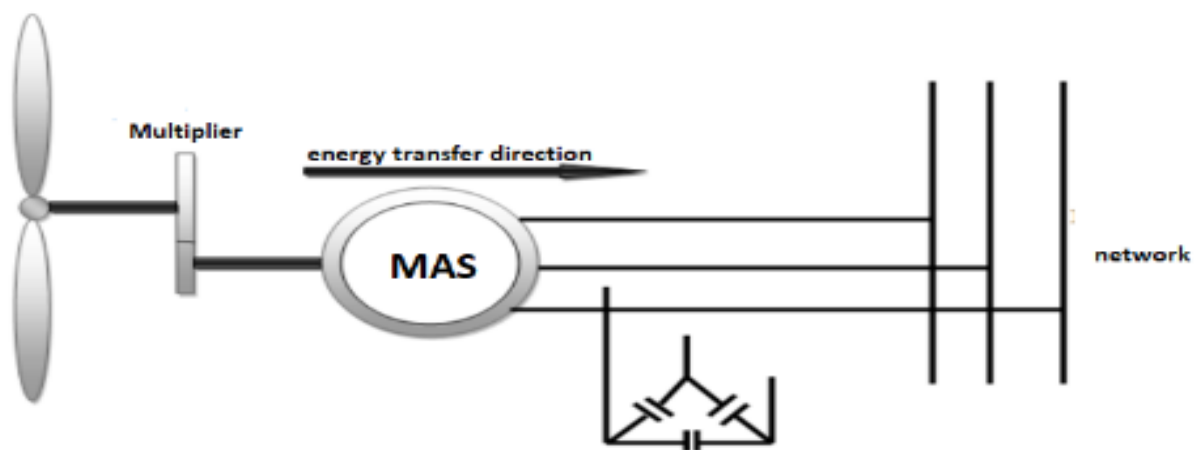


Fig.I.13: Asynchronous machine connected directly to the grid [29]

V.2.Variable Speed Systems

Variable speed wind turbines (VSWTs) have become the most dominant type among the installed wind turbines during the last 10 years [29]. Characteristic for variable speed wind turbines is that they are designed to operate with variable rotational speed. To optimize the power output according to the wind conditions, it is desirable to be able to adjust the speed of the

wind turbine. The idea is to create a generator with a fixed frequency and variable speed. The variable-speed generator allows operation over a wide range of wind speeds, thus recovering maximum power while reducing noise pollution when operating at low wind speeds. With variable speed, the system is regulated so that for each wind speed, the wind turbine operates at maximum power. This is the principle of Maximum Power Point Tracking (MPPT).

Several generators can be used. In our work, we will study and analyse an energy conversion chain based on a permanent magnet synchronous generator (PMSG), offering the possibility of direct coupling between the wind turbine rotor and the PMSG without a speed reducer (see figure below). This technology solves the problems of wind turbines operating at low speeds.

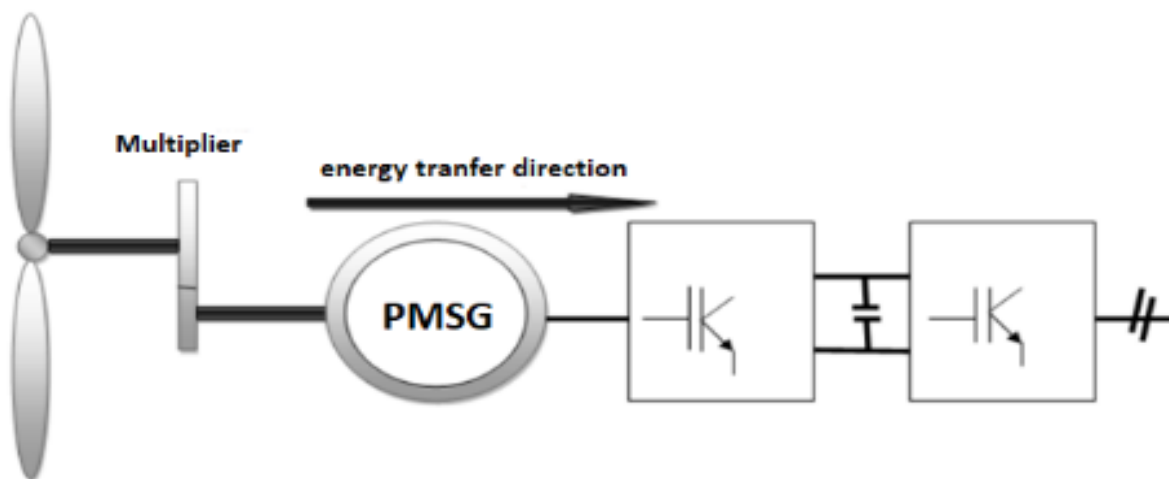


Fig.I.14: Wind energy system based on the permanent magnet synchronous machine

VI. Conclusion

In this chapter, we have given a brief description and some basic notions of wind turbine technologies, with emphasis on the different types of turbines. An aerodynamic study of horizontal axis turbines has also been made. The behaviour of different wind turbine configurations was investigated. The next chapter will be devoted to the presentation and mathematical modelling of the various parts making up a wind energy conversion chain based on a PMSG operating at variable speed. Next, we will develop the proposed approaches for controlling the wind energy conversion system.



CHAPTER II

Modeling and Feedback Linearization control of WECS in autonomous mode



I. Introduction

Among the various types of available wind turbines, the wind energy conversion systems (WECS) based permanent magnet synchronous generator (PMSG) are widely for variable speed wind turbine systems because of their simple mechanical structures, their reliable operations, their medium and high power, their energy efficiency and except initial installation costs [31]. The most important issue in the use of wind energy conversion systems is to ensure maximum power extraction in terms of efficiency because the main problem with wind power systems is the major discrepancy between the irregular nature of the primary source (wind speed is a random, highly non-stationary process with turbulence and extreme variations) and the power quality [32]. This chapter deals with the feedback linearization control (FLC) of PMSG based variable speed wind turbine power system. Because the WECS based PMSG is a nonlinear system, the system is globally linearized based the feedback linearization method, and the maximum power point tracking control is obtained. The autonomous wind power systems are isolated power producing systems connected to a local grid [32]. This chapter will focus on the modelling and performance analysis of FLC control strategies for maximum power extraction of the variable-speed autonomous WECS based on PMSG under different stochastic wind speeds. The wind system structure adopted in our study consists of a 3KW three-bladed wind turbine.

II. Model of the Wind Energy Conversion System

II.1. Aerodynamic Part

Wind energy is captured and transformed into mechanical energy through the wind turbine blades and then transformed into electrical energy by the PMSG. The variable speed with constant frequency adjustment method is mainly adopted when the PMSG wind energy conversion system changes widely between the cut-in wind speed and the optimal wind speed. The maximum wind energy conversion and the optimal wind energy coefficient are obtained with adjusting the rotor speed of the generator [24]. The diagram of a PMSG wind energy conversion system is illustrated in Fig. II.1.

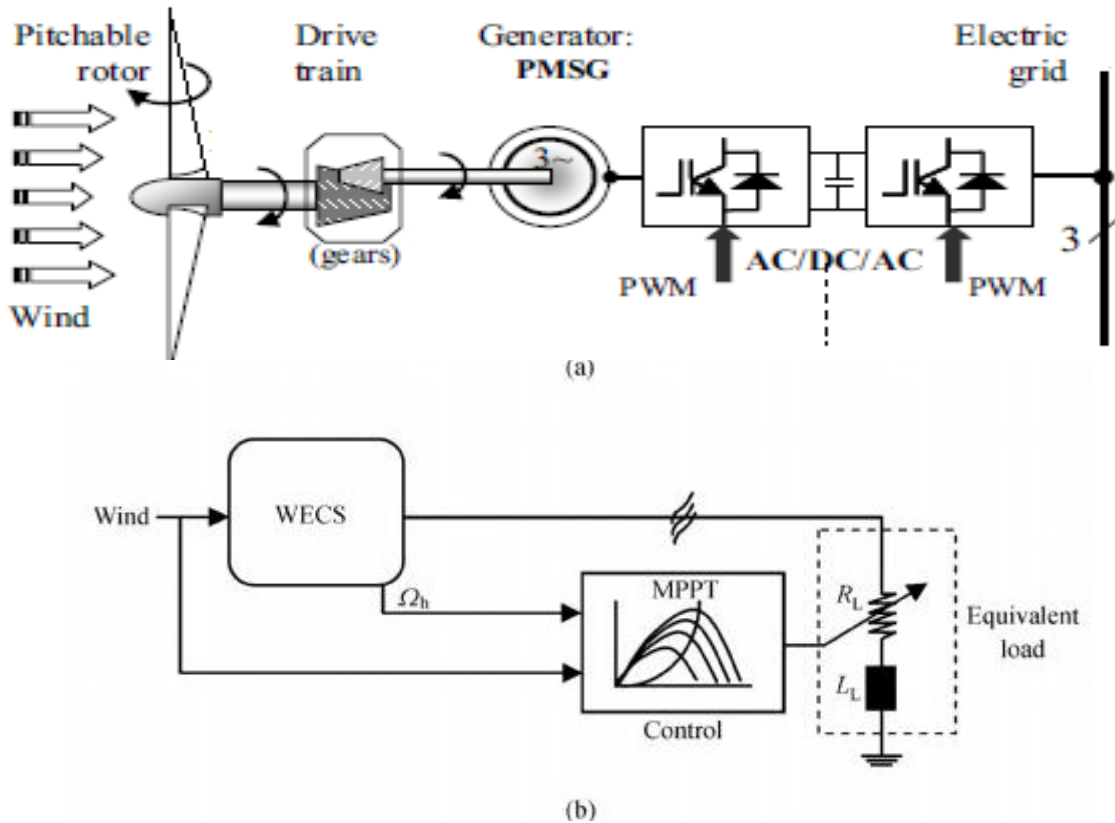


Fig.II.1: Block diagram of Permanent magnet synchronous generators in WECS systems [33];
 (a) Complete and (b) Equivalent diagram.

II.1.1. Model of the wind

It is very important for the wind industry to be able to describe the variation of wind speeds under optimal conditions. Wind is the main source of energy to operate a wind turbine, so it is necessary to know its mathematical model [34]. A typical (stochastic) wind model representing the energy of the wind source will be established to test different control strategies in the presence of turbulence. In our study, the evolution of wind speed as a function of time is modeled by an analytical function or generated by a statistical law from measurement data for a given site (climatic and geographical data). Wind speed signal is thus modeled by a superposition of several harmonics, in accordance with: [24]

$$V_w(t) = A + \sum_{k=1}^i a_k \sin(\omega_k t) \quad (\text{II.1})$$

With A : the mean value of the wind speed; a_k and ω_k : are respectively the amplitude and pulsation of the harmonic of order k and i : the rank of the last harmonic used in the calculation of the wind profile. In our work; the wind speed profile is given by:

$$V(t) = 7.5 + 0.2 \sin(0.1047t) + 2 \sin(0.2665t) + \sin(1.2930t) + 0.2 \sin(3.6645t) \quad (II.2)$$

II.1.2. Aerodynamic model of the wind turbine

A wind turbine converts kinetic energy from the wind to drive the wind turbine rotor, which is connected to a generator producing electricity. The maximum power output from the wind turbine is limited by the power coefficient C_p which is a function of the tip speed ratio λ .

The expression for power captured by the wind turbine is defined as follows:

$$P_w = \frac{1}{2} \cdot \rho \cdot A \cdot V^3 \quad (II.3)$$

Where ρ : Air density (estimated 1.25Kg/m^3); A : is the circular area swept by the turbine [m^2] and V : velocity wind.

The mechanical power extracted from the wind (Aerodynamic power) appearing on the turbine rotor is defined as follows:

$$P_{aer} = C_p \cdot P_w = \frac{1}{2} \cdot C_p(\lambda, \beta) \cdot A \cdot \rho \cdot V^3 \quad (II.4)$$

$C_p(\lambda, \beta)$: The aerodynamic power coefficient of the turbine (β : Blade pitch angle; λ : the tip speed ratio (TSR)). The power coefficient evolved as a function of λ for different values of β , The maximum power is obtained for an optimal tip speed ratio and a fixed-pitch turbine $\beta = 0$.

The aerodynamic torque coefficient $C_T(\lambda)$ can generally be described by a polynomial function (polynomial regression) of the specific speed λ . In our study, it is defined by:

$$C_T(\lambda) = a_6 \lambda^6 + a_5 \lambda^5 + a_4 \lambda^4 + a_3 \lambda^3 + a_2 \lambda^2 + a_1 \lambda + a_0 \quad (II.5)$$

With:

$$a_6 = -4,4 \cdot 10^{-7}; a_5 = 1,3027 \cdot 10^{-5}; a_4 = -6,5416 \cdot 10^{-5}; a_3 = -9,7477 \cdot 10^{-4}; a_2 = 0,0081; a_1 = -0,0013; a_0 = 0,0061$$

The pitch angle is considered fixed [9].

To obtain maximum power from the PMSG-WECS, the speed ratio at the tip of the blade must be adjusted. To do this, the rotor speed must be regulated according to the variation in wind speed, so that the wind energy system can operate correctly [9]. The theoretical upper limit of the power coefficient C_{p_max} is given by Betz's limit [9]:

$$C_{pmax} = \frac{16}{27} = 0.59 \quad (II.6)$$

This limit is in reality never reached, and the best machines with horizontal axis, two-blade or three-blade, are at 60-65% of the BETZ limit because of aerodynamic losses, which depend on rotor design and construction (number of blades, weight, rigidity, etc.) [9]. Then we deduce the aerodynamic efficiency by:

$$\eta = \frac{16}{27} C_{pmax} \quad (II.7)$$

C_{pmax} : being the maximum value of the power coefficient C_p . This value is associated with a nominal specific speed λ_{opt} for which the turbine has been dimensioned according to a nominal wind speed V_n and a nominal rotation speed Ω_{tn} ($\lambda_{opt}=7$).

The wind turbine provides the mechanical torque of the shaft according to the expression of the wind torque by:

$$\Gamma_w = \frac{P_w}{\Omega_t} = \frac{1}{2} \rho \cdot \pi \cdot R^2 \cdot V_w^2 \cdot C_\Gamma(\lambda) \quad (II.8)$$

With
$$C_p(\lambda) = C_\Gamma(\lambda) * \lambda \quad (II.9)$$

The tip speed ratio can be expressed as: $\lambda = \frac{\omega_r R}{V}$, where ω_r is the rotational speed of the turbine on the low-speed side of the gearbox.

In the context of our work, the aerodynamic torque of a 3kW wind turbine is approximated by the following equation:

$$\Gamma_w = d_1 V^2 + d_2 V \Omega_t + d_3 \Omega_t^2 \quad (II.10)$$

$$\text{With: } \begin{cases} d_1 = \frac{1}{2} \cdot \pi \rho R^3 \alpha_0 \\ d_2 = \frac{1}{2} \cdot \pi \rho R^4 \alpha_1 \\ d_3 = 1/2 \cdot \pi \rho \alpha_2 \end{cases} ; \begin{cases} \alpha_0 = 0.1253 \\ \alpha_1 = -0.0047 \\ \alpha_2 = -0.0005 \end{cases}$$

Where Γ_w : is the aerodynamic torque, Ω_t : Angular velocity and V : wind speed.

II.2. Modeling of mechanical part

The mechanical system of the wind turbine is composed of four parts and can be represented as shown on the figure below [35].

Let's consider a mechanical part of the turbine comprises with three steerable blades of length R. They are attached to a drive shaft rotating at a speed Ω_{turbine} and which is connected to a gearbox of gain G. This gearbox drives the electric generator (see Figure below)

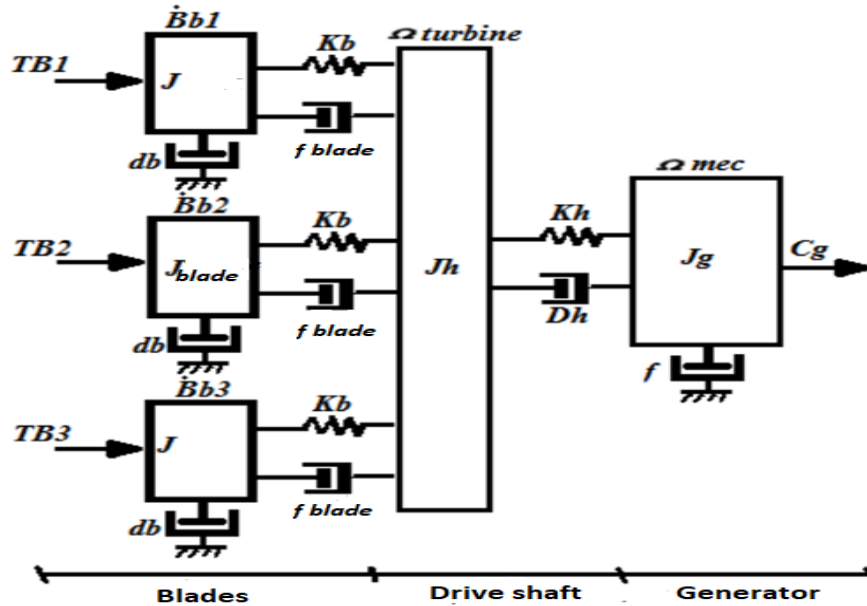


Fig. II.2: Mechanical system of the turbine

The mechanical system of the wind turbines plays a big role in the energy transformation. The essential and simplifying assumptions for the mechanical modelling of the turbine are: [35]

- The three blades are considered identical in design and therefore have the same parameters:
 - the same inertia J_{blade}
 - the same elasticity K_b
 - the same coefficient of friction with respect to air d_b
- The blade drive shaft is characterized by: the inertia J_h ; the elasticity K_h and the friction coefficient to the gearbox d_h
- The speed multiplier, of gain G.
- The rotor of the generator has: inertia J_g ; a friction coefficient d_g

This rotor transmits a torque (Γ_g) to the electric generator and rotates at a speed noted Ω_{mec} . If we consider a uniform distribution of wind speed on all blades, and therefore equality of all thrust forces ($TB1 = TB2 = TB3$), then we can consider all three blades as a single mechanical system, characterized by the sum of all mechanical characteristics [35]. On the other hand, the aerodynamic design of the blades means that their coefficient of friction with respect to the air is

very low and can be ignored. Similarly, as the turbine speed is very low, friction losses are negligible compared to friction losses on the generator side. The result is a mechanical model with two rotating masses (Fig. II.3), driven by aerodynamic torque [24].

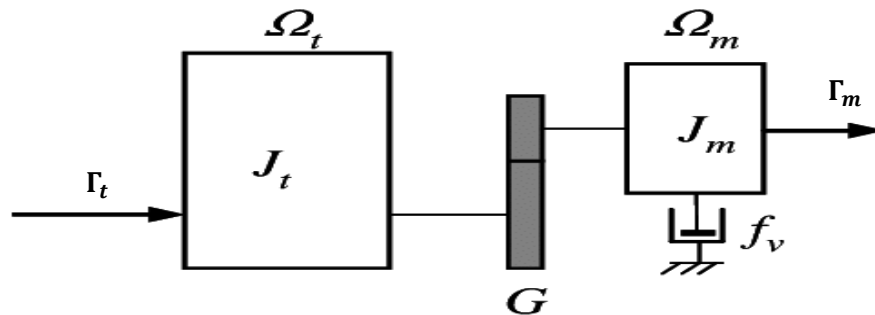


Fig.II.3: Simplified turbine model

II.2.1 Model of the multiplier

A gearbox is often used in a wind turbine to increase the rotational speed from a low-speed main shaft to a high-speed shaft connecting with an electrical generator (see figure below).

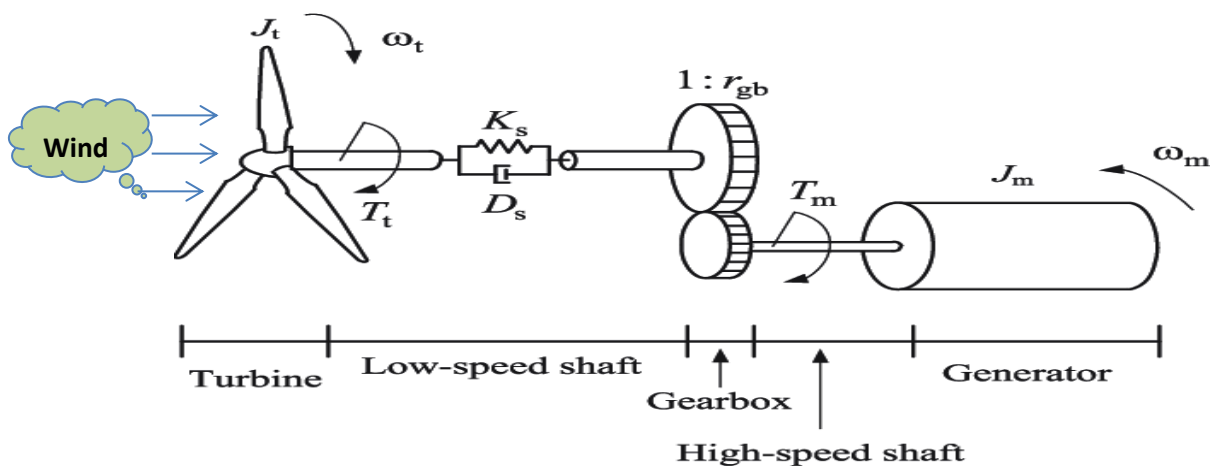


Fig.II.4: Diagram of the WECS system based on PMSG.

This speed multiplier G is mathematically modelled by the following [24]:

$$\begin{cases} G = \frac{\Omega_{mec}}{\Omega_{tur}} \\ G = \frac{\Gamma_{aer}}{\Gamma_g} \end{cases} \quad (II.11)$$

The synoptic diagram of the dynamic model of the turbine based on these equations is given in the following figure.

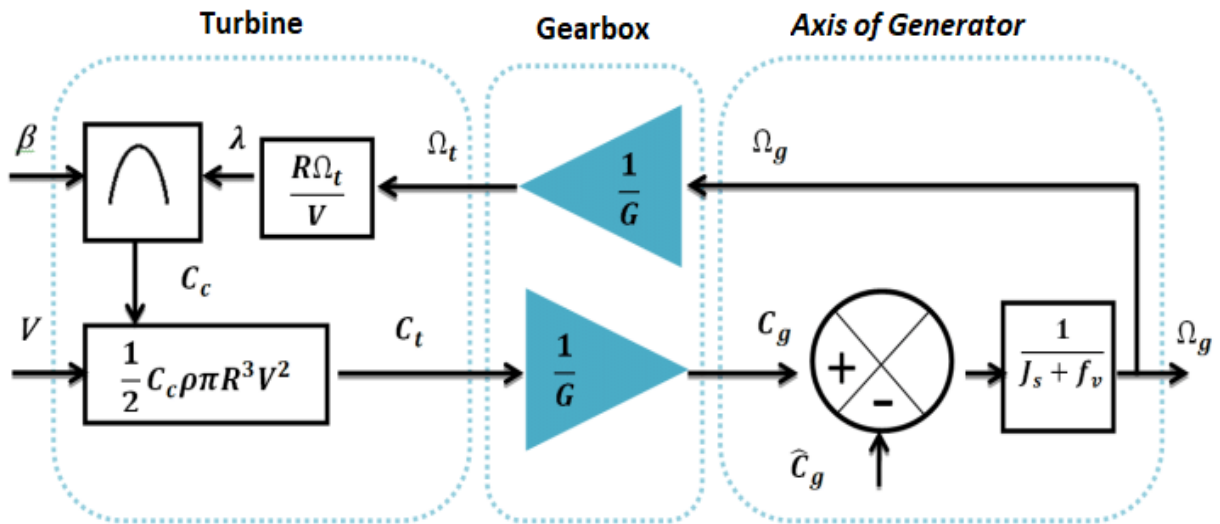


Fig.II.5: Block diagram of turbine model

II.2.2 Modeling of the Permanent Magnet Synchronous Generator

Electrical generator is the main device converting wind energy into electric power. The permanent magnet synchronous generator (PMSG) has the property of self-excitation, which allows an operation at a high power and a high efficiency [36]. The structure of PMSG comprises a three-phase winding in the stator. The rotor excitation is created by permanent magnets in the rotor. These magnets are assumed to be rigid and to have a permeability close to that of air. Its operating principle is based on synchronization between the magnetic fields produced by the stator and the rotor. In order to accurately reproduce the generator's behaviour in transient regimes, we are building a dynamic model of PMSG. The representation of the variables in the Park reference frame is shown in the following figure, where axis (d) is the directional position of the permanent magnets and axis (q) is in quadrature with direction (d).

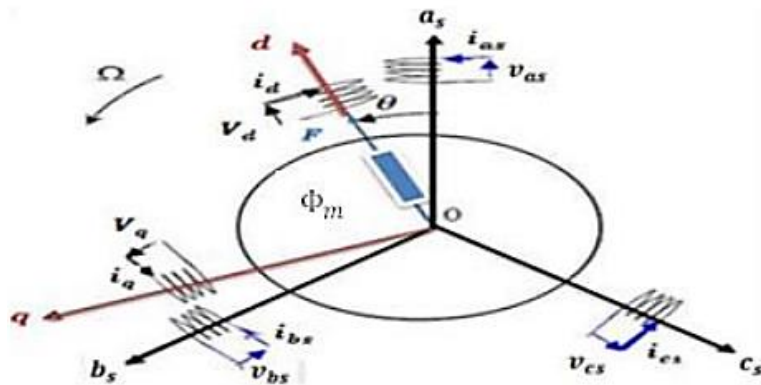


Fig.II.6: Transition from a three-phase system (permanent magnet synchronous

The following simplifying assumptions are used to model the PMSG [37]:

- The absence of saturation in the magnetic circuit
- The sinusoidal distribution of the MMF created by the stator windings
- Hysteresis is neglected with eddy currents and skin effect
- The notching effect is negligible
- Winding resistance does not vary with temperature

a. Mechanical part (Dynamic equation of the drive shaft)

The mass of the wind turbine is transferred to the turbine shaft in the form of inertia note: $J = J_{turbine}$ and includes the mass of the blades and the mass of the turbine rotor. The proposed mechanical model considers the total inertia J consisting of the inertia of the turbine carried over to the generator rotor and the inertia of the latter [38]:

$$J = J_{turbine} + J_{generator} \tag{II.12}$$

The fundamental equation of dynamics allows us to determine the evolution of mechanical velocity from the total mechanical torque Γ_m applied to the rotor [38]:

$$J_h \frac{d\Omega_h}{dx} = \frac{\eta}{G} \Gamma_m - \Gamma_g \tag{II.13}$$

With $\Omega_h = \Omega_r \times G$ and where J_h : Is the moment of inertia brought back to the high-speed shaft. Ω_h, η, Γ_g and G are respectively, generator speed, efficiency, electromagnetic torque and multiplier ratio.

b. Electricals equations

The electrical equations of the electric machines in the fixed reference frame linked to the stator are described by [39]:

$$\begin{bmatrix} V_{sa} \\ V_{sb} \\ V_{sc} \end{bmatrix} = R_s \begin{bmatrix} I_{sa} \\ I_{sb} \\ I_{sc} \end{bmatrix} + \frac{d}{dt} \begin{bmatrix} \psi_{sa} \\ \psi_{sb} \\ \psi_{sc} \end{bmatrix} \tag{II.14}$$

With: R_s : Resistance of the stator phases; $[V_{sa} V_{sb} V_{sc}]^T$: Voltages of the stator phases; $[I_{sa} I_{sb} I_{sc}]^T$: Stator phase currents and $[\psi_{sa} \psi_{sb} \psi_{sc}]^T$: The total flux through the stator.

The equivalent electrical model of PMSG /Equivalent Load in the (d,q) is represented by the electrical diagram in (see Fig. II.8)

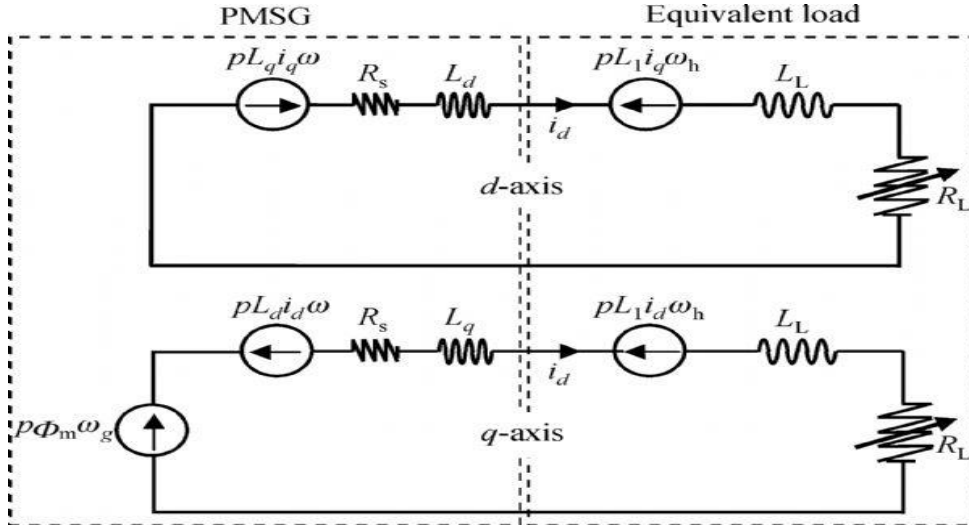


Fig.II.7: Equivalent Electrical model in reference frame (d, q) [40]

The PMSG dynamic equations are expressed in the d-q reference frame by the following equation [40]:

$$\begin{cases} V_{sd} = -R_s i_{sd} - L_d \frac{d}{dt} i_{sd} + \omega_e L_q i_{sq} \\ V_{sq} = -R_s i_{sq} - L_q \frac{d}{dt} i_{sq} + \omega_e (L_d i_{sd} - \Phi_m) \end{cases} \quad (\text{II.15})$$

with R_s : Stator resistance per phase; L_d, L_q : Direct-axis and quadrature stator inductances respectively; V_{sd}, V_{sq} : Two-phase stator voltages in frame (d-q); i_{sd}, i_{sq} : Two-phase stator currents in frame (d-q); ω_e : Electrical angular speed of the PMSG and Φ_m : Amplitude of the flux created by the permanent magnets through the stator windings.

The electrical state model is given as follows:

$$\begin{cases} \frac{d}{dt} i_d = -\frac{R_s + R_L}{L_d + L_L} i_d + \frac{P(L_q - L_L)}{L_d + L_L} i_q \Omega_h \\ \frac{d}{dt} i_q = -\frac{R_s + R_L}{L_q + L_L} i_q + \frac{P(L_d + L_L)}{L_q + L_L} i_d \Omega_h + \frac{P\Phi_m}{L_q + L_L} \Omega_h \end{cases} \quad (\text{II.16})$$

Where R_L : Equivalent inductance; P : number of pole pairs and Φ_m : Magnet flux. The relationship between the electric speed and the mechanical speed can be expressed as: $\omega_e = \frac{P}{2} \Omega_m$.

The generator torque equation is given by:

$$\Gamma_{em} = P\Phi_m i_q = P[(L_d - L_q)i_d i_q - \Phi_m i_q] \quad (\text{II.17})$$

Choosing, respectively the state vector $x(t)$, the input signal $u(t)$ and the desired output $y(t)$ as [11]:

$$\begin{cases} x(t) = [x_1(t) x_2(t) x_3(t)]^T \equiv [i_d(t) i_q(t) \Omega_h(t)]^T \\ u(t) = [u_1(t) u_2(t)]^T \equiv [R_L(t) v]^T \\ y(t) = \Omega_h \end{cases} \quad (\text{II.18})$$

The nonlinear state-space model of the PSMG is given by [41]:

$$\begin{cases} \dot{x}(t) = f(x) + g(x(t))u(t) \\ y(t) = h(x(t)) \end{cases} \quad (\text{II.19})$$

where :

$$\begin{cases} f(x) = \begin{bmatrix} \frac{1}{L_d + L_L} (-R_s x_1 + p(L_q - L_L)x_2 x_3) \\ \frac{1}{L_q + L_L} (-R x_2 - p(L_d + L_L)x_1 x_3 + p\Phi_m x_3) \\ \frac{1}{J} (d_1 v^2 + d_2 v x_3 + d_3 x_3^2 - p\Phi_m x_2) \end{bmatrix} \\ g(x) = \begin{bmatrix} -\frac{1}{L_d + L_a} & -\frac{1}{L_q + L_L} x_2 & 0 \end{bmatrix} \\ h(x) = x_3 = \Omega_h \end{cases} \quad (\text{II.20})$$

And: $u = R_s$

The parameters are defined by: $d_1 = \frac{\eta\rho\pi R^3}{2i} q_0$, $d_2 = \frac{\eta\rho\pi R^4}{2i^2} q_1$, $d_3 = \frac{\eta\rho\pi R^5}{2i^3} q_2$

III.MPPT Controller Based on Feedback Linearization Method

III.1. Maximum Power Point Tracking Algorithms

The MPPT (Maximum Power Point Tracking) technique is a highly reliable control method and simple to implement. It consists in tracking the maximum power point of a generator for a variable source (e.g. wind speed in the case of a wind turbine). The aim is to determine the speed of the wind turbine that will produce the maximum power [1-30]. Several MPPT techniques are used to extract maximum power from variable-speed WECS, which requires varying rotor speed in response to changes in wind speed.

Two main MPPT techniques are used to detect and track the maximum power point (MPP); the indirect power controller (IPC) and the direct power controller (DPC). Recently, other MPPT techniques based on meta-heuristic optimization algorithms have been used. The following figure shows a general classification of the various MPPT techniques [9].

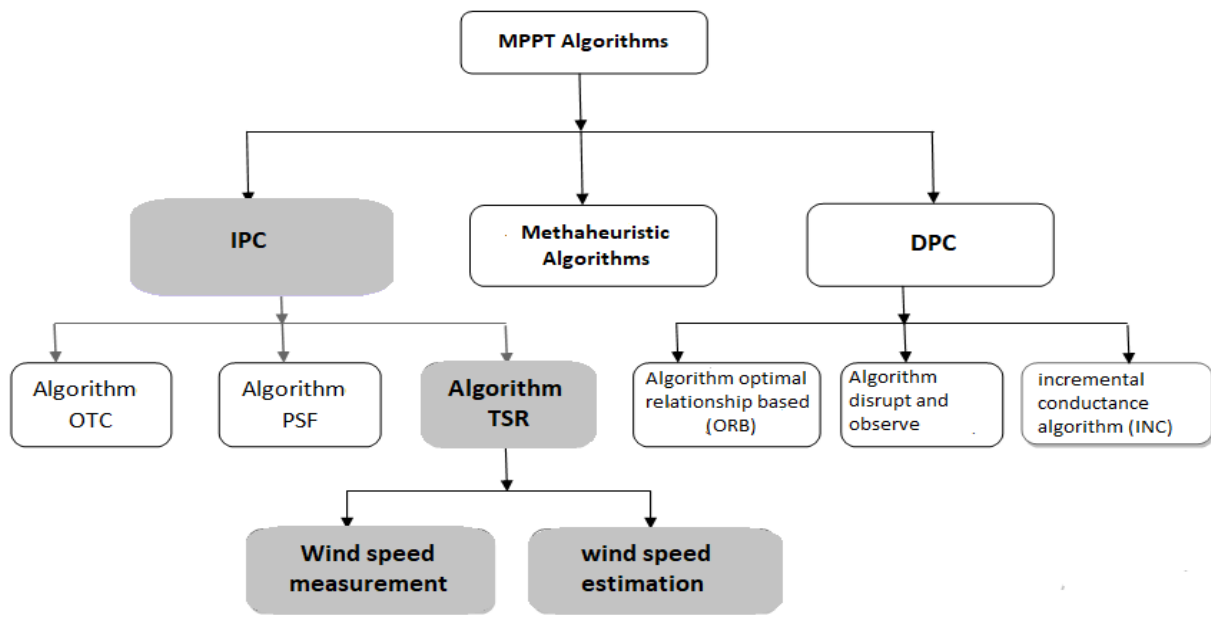


Fig.II.8 : Classification of different MPPT techniques

III.1.1 MPPT algorithms based on IPC

The TSR algorithm is one of three in the group of IPC algorithms [9]. This method needs a wind velocity sensor to change the gear ratio and alter the speed of the turbine rotor to drive the generator. However, wind turbulence can cause the wind speed sensor to be inaccurate, leading to deviation when extracting the maximum power of WECS. The additional two MPPT methods are power signal feedback algorithms (PSF) and the torque optimization algorithm (OT). There is no need for an anemometer, but the manufacturer must provide exact wind speed parameters.

a- MPPT with the optimal specific speed (Tip Speed Ratio - TSR)

In our work, we will use MPPT based on TSR technique to control the PMSG-WECS system. This is a straightforward strategy to be executed as only the measured wind speed is required for the input of the MPPT controller [30-43]. It's necessary to regulate the turbine power to extract a maximum wind power. The turbine power P_t is depend to the wind speed v and the power coefficient C_p . In order to maximize the turbine power, we have to research the optimum one. The objective is to keep the TSR at its optimum value by measuring the speed of the turbine and the instantaneous speed of the wind. The aim is to remain constantly at the point $(\lambda_{opt}, C_{pmax})$. This

involves varying the turbine speed Ω_h according to variations in wind speed v . $[\lambda_{opt} = 7, C_{pmax} = 0.475]$.

For the speed control of the synchronous generator with permanent magnets, the reference speed of the wind turbine is obtained by:

$$\Omega_h^* = \frac{\lambda_{opt} \cdot V}{R_t} \tag{II.21}$$

Figure II.12 shows the schematic diagram of PMSG-WECS using the TSR method.

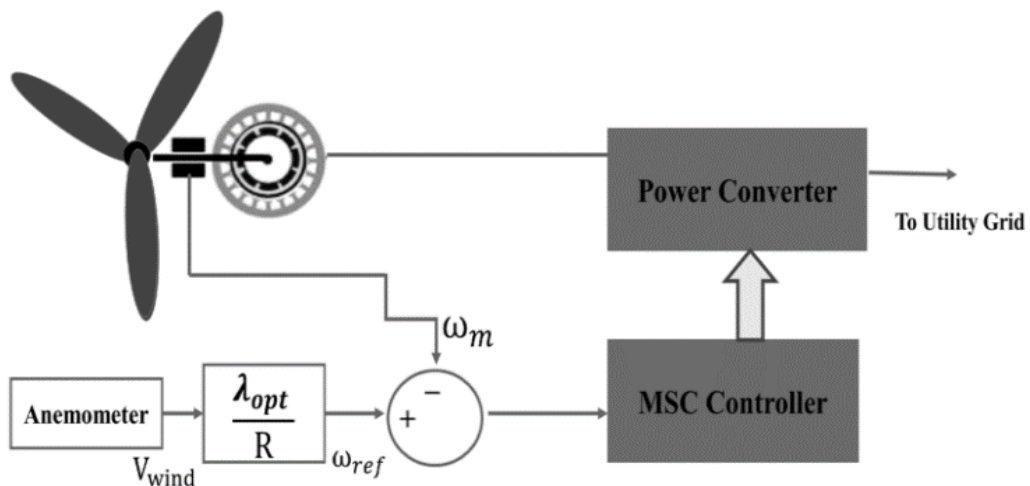


Fig.II.9: MPPT with the optimal specific speed (TSR).

b- MPPT with the power profile (PSF)

Figure below explains the PSF algorithm diagram. This technique is comparable to the OT algorithm, which frequently has high inertia when wind speed is low but reasonable cost and quick processing speed. In this method Wind speed and torque speed are used as input signals, and the controller corrects the difference between the optimal and actual power of the system [40].

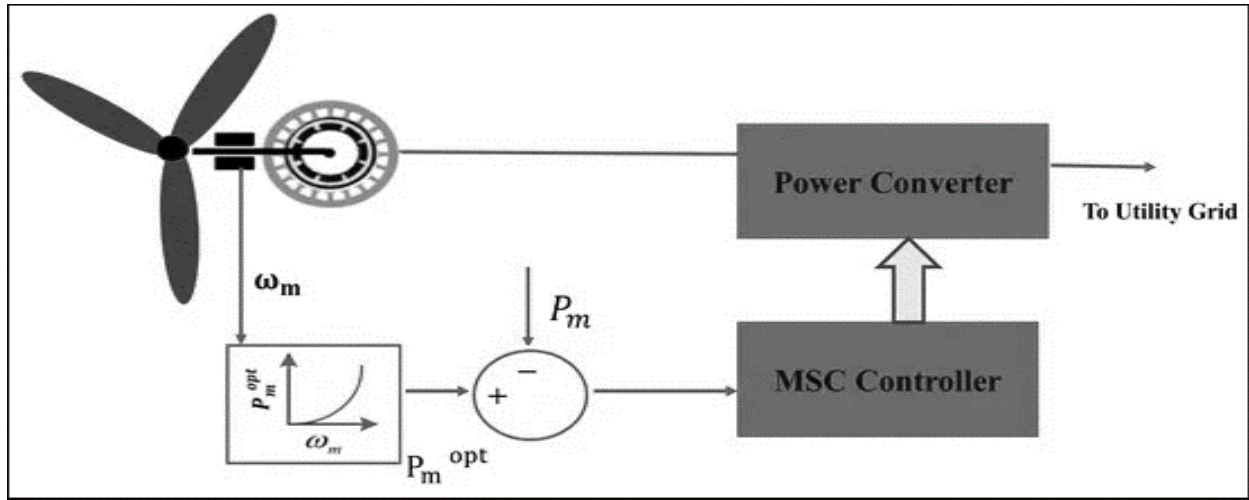


Fig.II.10: Diagram of PSF MPPT algorithm.

c- MPPT with Optimal Torque Control (OT)

Without wind speed measurements, the goal of maximum conversion efficiency can be achieved by producing an optimum torque reference based on just a few turbine parameters and simple generator speed measurements Ω_h , as illustrated in Figure II.14.

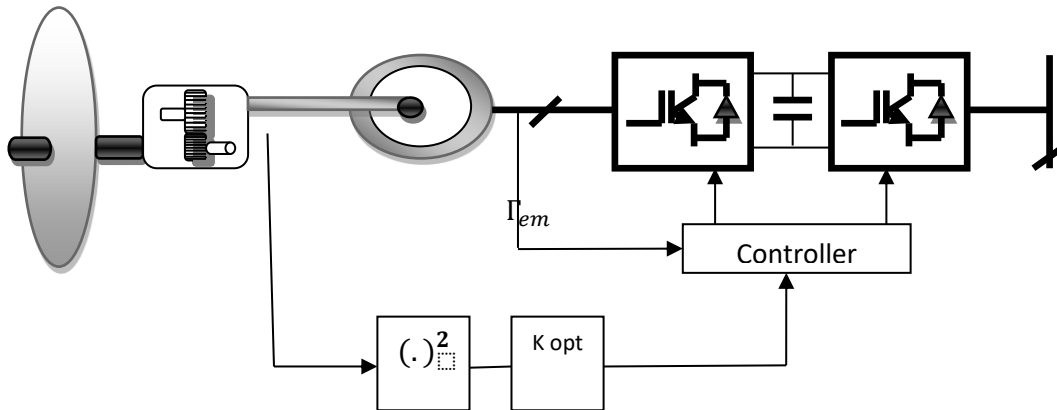


Fig II.11 MPPT based Optimal torque control (OTC).

$$\Gamma_{em}^* = K_{opt} \Omega_{h-opt}^2 \tag{II. 22}$$

With:

$$\begin{cases} K_{opt} = \frac{1}{2} \frac{C_{p-opt}(\Omega_h) * \rho * \pi * R^5}{\lambda_{opt}^3(\Omega_h) * G^3} \\ \Omega_{l-opt} = \frac{v * \lambda_{opt}}{R} \\ \Omega_t = \frac{\Omega_h}{G} \end{cases} \tag{II. 23}$$

The power extracted by a wind turbine is expressed as:

$$P_m = \frac{1}{2} * \rho * \pi * R^2 * v^3 * C_p(\lambda) \quad (\text{II. 24})$$

From the expression for the power extracted by a wind turbine, it follows that:

$$P_m = \frac{1}{2} * \rho * \pi * R^2 * v^3 * C_p(\lambda) = \frac{1}{2} * \frac{C_p(\lambda)}{\lambda^3} * \rho * \pi * R^5 * \Omega_l^3 \quad (\text{II. 25})$$

Replacing $\lambda(t)$ by λ_{opt} and C_p by $C_p(\lambda_{opt})$ with; gives the reference value of the power for the second region of the power-wind speed curve:

$$P_m = P_m^* = K * \Omega_l^3 \quad (\text{II. 26})$$

Where:

$$K = \frac{1}{2} \frac{C_p(\lambda_{opt})}{\lambda_{opt}^3} \rho \pi R^5 \quad (\text{II. 27})$$

In this method, the torque of the generator is controlled at its optimum in order to obtain the maximum value of the power maximum value of the power coefficient and, consequently, maximum energy efficiency.

IV.PSMG-WECS Controller Design Based on Feedback Linearization

The aim is to maximize the power extraction when the WECS operates in the partial-load regime. This is accomplished by controlling the shaft speed. Feedback linearization is a common strategy employed in nonlinear control to control nonlinear systems . Because PSMG-WECS is a strong multiplication nonlinear system, the system is globally linearized based the feedback linearization method, and the maximum power point tracking control law is obtained. The goal of feedback linearization is to produce a transformed system whose states are the output and its first (n-1) derivatives. For this, we use the Lie derivative [11]

To simplify the complexity of the complete non-linear system we assume that the wind speed varies slightly from one operating point to another. These results in a simplified system presented by a single input signal $u = [R_L V]$, $X = [x_1 x_2 x_3]^T = [i_d i_q \Omega_h]^T$ and the desired output is Ω_h (see eq. II. 19; eq. II.20). The system given by Eq. (II.19 and II.20) is considered as non-linear with smooth functions whose synthesis of feedback linearization control is possible to make the system linear. The approach involves transforming a nonlinear control system into an equivalent

linear control system through a change of variables and a suitable control input. To calculate the Lie derivatives, we determine the relative system degree:

$$\begin{cases} L_f h(x) = d_1 v^2 + d_2 v x_3 + d_3 x_3^2 - d_4 x_2 \\ L_g L_f h(x) = -d_4 a_3 x_2 \neq 0 \end{cases} \quad (II.28)$$

Since $L_g L_f^n h(x) \neq 0$, with $n = 1$ the relative of the system is $r = n + 1 = 2$. This means that only a *partial* linearisation is possible. The linearization affects only the system dynamics that are responsible for the input/output mapping, while the rest of the dynamics are internal and they do not influence the input-output mapping.

In order to bring the system in the *normal form*, a coordinate transform, fulfilling the diffeomorphism condition, must be found:

$$\frac{\partial z_3}{\partial x_1} g_1 + \frac{\partial z_3}{\partial x_2} g_2 + \frac{\partial z_3}{\partial x_3} = \frac{\partial z_3}{\partial x_1} a_3 x_1 + \frac{\partial z_3}{\partial x_2} a_3 x_2 = 0 \quad (II.29)$$

Where $a_3 = -\frac{1}{(L_d + L_f)}$. The condition is fulfilled for $z_3 = a_3 x_1 / x_2$. The coordinate transform that leads to a partial linearization of the system is [46]:

$$z = \phi(x_1, x_2, x_3) = \begin{bmatrix} \phi_1(x_1, x_2, x_3) \\ \phi_2(x_1, x_2, x_3) \\ \phi_3(x_1, x_2, x_3) \end{bmatrix} = \begin{bmatrix} x_3 \\ d_1 v^2 + d_2 v x_3 + d_3 x_3^2 - d_4 x_2 \\ a_3 \frac{x_1}{x_2} \end{bmatrix} \quad (II.30)$$

The direct coordinates transform is:

$$\begin{cases} z_1 = h(x) = x_3 \\ z_2 = L_f h(x) = d_1 v^2 + d_2 v x_3 + d_3 x_3^2 - d_4 x_2 \\ z_3 = a_3 \frac{x_1}{x_2} \end{cases} \quad (II.31)$$

And the inverse coordinates transform is given by :

$$\begin{cases} x_1 = a_3 z_3 \cdot \frac{d_1 v^2 + d_2 v z_1 + d_3 z_1^2 - z_2}{d_4} \\ x_2 = \frac{d_1 v^2 + d_2 v \cdot z_1 + d_3 z_1^2 - z_2}{d_4} \\ x_3 = z_1 \end{cases} \quad (II.32)$$

The control input will be:

$$u = \frac{1}{L_g L_f h(x)} (-L_f^2 h(x) + u_v) \quad (II.33)$$

Where:

$$\begin{cases} L_f^2 h(x) = -d_4 \cdot f_2 + (d_2 v + 2d_3 x_3) \cdot f_3 \\ L_g L_f h(x) = -d_4 a_3 x_2 \end{cases} \quad (II.34)$$

The control input has a state feedback component, $L_f^2 h(x)$ and $L_g L_f h(x)$ and a component u_v are Lie derives, which forces a dynamic linear input/output mapping. The latter is a state feedback control, as shown in Fig. II.1.

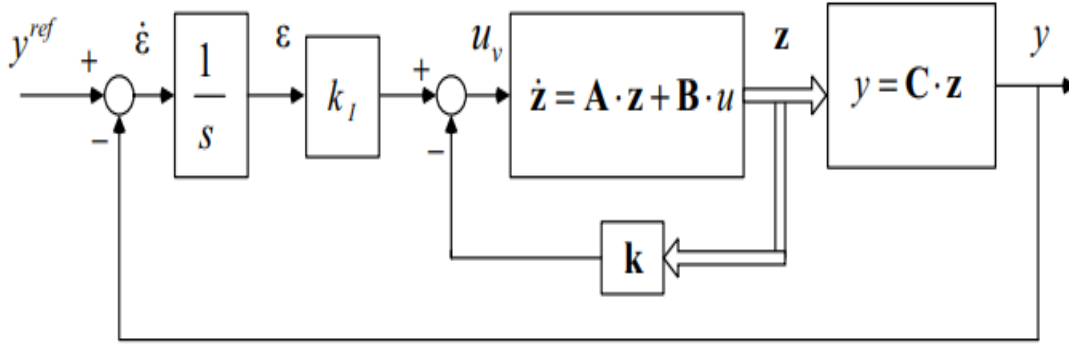


Fig.II.12: State-feedback control.

The control input u_v is calculated by:

$$u_v = -[k_1 \ k_2 \ -k_I] \begin{bmatrix} z_1 \\ z_2 \\ \epsilon \end{bmatrix} \quad (II.)$$

And k_1, k_2, k_I are calculated using a pole-placement technique. In our work, we use these parameters values: $k_1 = 4000; k_2 = 136; k_3 = 40000$.

As the aim of controlling the wind energy conversion system is to extract the maximum wind, which will be achieved by driving the generator at a speed Ω_h that asymptotically should asymptotically follow the optimal reference speed λ_{opt} . The output tracking error and its associated vector are defined by:

$$\epsilon = y^{ref} - y \quad with \quad \begin{cases} y^{ref} = \Omega_t^{ref} = \frac{\lambda_{opt} \cdot V}{R} \\ y = \frac{\Omega_h}{G} \end{cases} \quad (II.29)$$

The block diagram of the maximum power extraction using feedback linearization control is presented in Fig II.10.

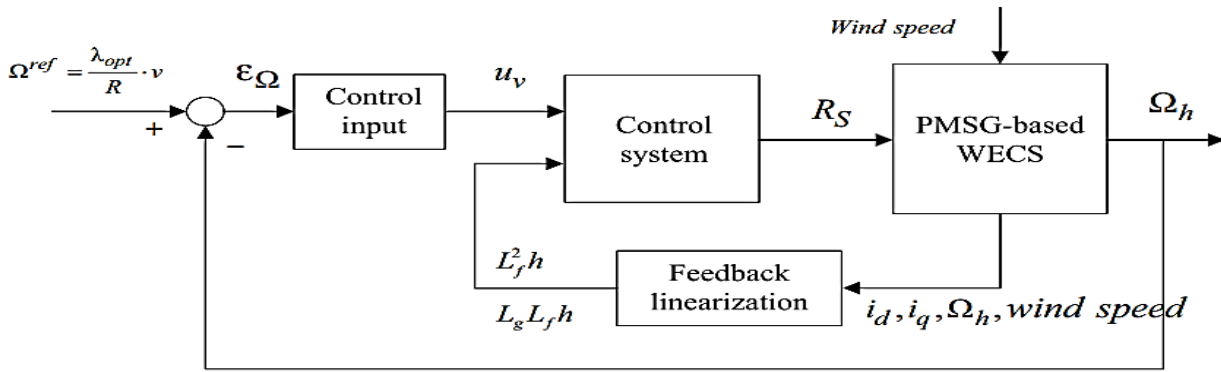


Fig.II.13: Feedback linearization control of PMSG-based WECS

V.MPPT-TSR control based on a PI controller

The PI controllers have been extensively used in the renewable energy conversion systems due to their satisfactory behaviour in most of the control processes, simple structure, and simple design procedure. The PI controller is used to reduce the error between the optimal speed reference and the applied speed. To determine the PI controller parameters (K_p, K_i and T_d), the Ziegler-Nichols method is used [24]. Figure below shows the diagram of TSR –MPPT technique for PMSG-WECS system control.

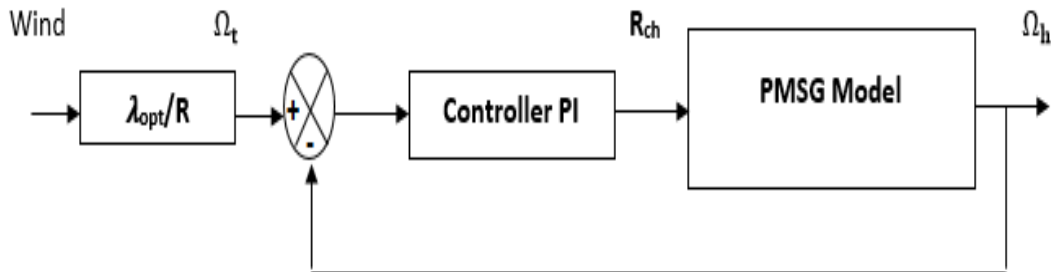


Fig.II.14: TSR control based on a PI controller for PMSG-WECS system.

- Calculate the gain (K_u) and the period (T_u) using Ziegler and Nichols method [4]

Firstly, the integral action and the derivative action are cancelled out. The proportional action is increased until the output signal of the closed loop oscillates in a maintained. This gain k_u is then noted as the maximum gain (or critical gain). We note the period of oscillation

of the signal. The parameters of the controller k_p, k_i and T_d are chosen by referring to the table below.

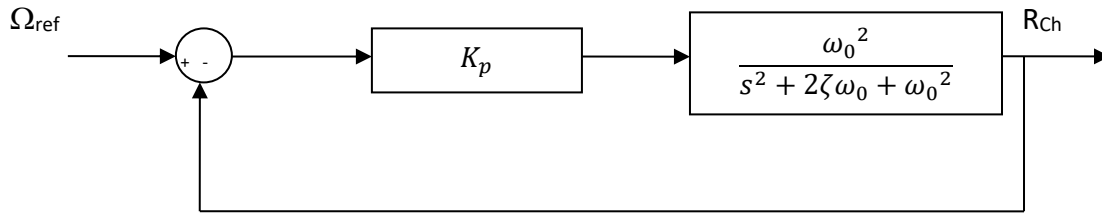


Fig.II.15: Mathematical calculation of (k_u) and (T_u)

The closed loop transfer function:

$$H_{BF} = \frac{R(S)}{Y(S)} = \frac{400k_p}{p^2 + 36p + 400k_p + 400} \quad (II. 37)$$

By applying criterion of to calculate the (k_u) for the given characteristic equation by: $p^2 + 36p + (400k_p + 400)$

$$\begin{cases} p^2 & 1 & (400k_p + 400) \\ p^1 & 36 & 0 \\ p^0 & (400k_p + 400) & 0 \end{cases}$$

So, $k_p = 1$ and $k_u = 1$. to calculate the period, we have $T_u = 0.26$ and

$$(j\omega)^2 + 36(j\omega) + (400k_p + 400) = 0 \quad \text{So: } \omega = 24.08 \text{ and the period: } T_u = \frac{2\pi}{\omega} = 0.26$$

$$\text{So: } (k_p = 1 \text{ and } T_u = 0.26)$$

VI. Conclusion

This chapter is devoted to Modeling and control of a wind power conversion system in autonomous mode based on a permanent magnet synchronous machine with the random nature of wind speed. The maximize energy captured from the wind of a grid-connected variable speed WECS based on a PMSG is also investigated. Because the WECS based on a PMSG is a strong multiplication nonlinear system, the system is globally linearized based the feedback linearization method, and the maximum power point tracking control law is obtained. To do this, we began by describing the three parts of the wind turbine conversion system (the mechanical part containing the turbine and generator shaft, and the electrical part representing the permanent magnet

machine model, operating in stand-alone mode). The modelling was carried out under a number of simplifying assumptions, resulting in a non-linear mathematical model that required the system to be linearized using the feedback linearization method.

In the following chapter, we will present the various simulation results obtained by the two proposed control approaches for capturing maximum power using variable wind speed. The two MPPT control structures are: PI controller and feedback linearization controller.



CHAPTER III

Results and interpretation



I. Introduction

The simulation is carried out for a small wind power conversion chain based on a synchronous generator with permanent magnet (PMSG) of 3KW having a maximum power coefficient $C_{P_{max}} \approx 0.476$ which corresponds to an TSR optimal $\lambda^* \approx 7$. We have started the simulation performance without MPPT technique then the simulation performance with MPPT technique based on PI controller and Feedback Linearization Control (FLC) respectively.

The PMSG based WECS modelled in Chapter 2, having parameters given in Table III.1, was designed with the FLC method. The controller imposes the generator speed in such a way that the system operates on the optimal regimes characteristic (ORC). The control input is the equivalent load resistance R_{ch} . The simulation steps are as follows:

A first test on the performance of the proposed controller with respect to the extraction of the maximum MPPT power is carried out under a typical wind profile (Figure III.11) having an average speed of 7 m/s and a sinusoidal spectrum. A second robustness test of the controller is carried out under an average speed of 7 m/s and an average turbulence intensity using the white noise spectrum (Figure III.20).

Turbine rotor	Training	PMSG	Torque coefficient parameters
$R_s = 2.5 \text{ m}$ $\rho = 1.25 \text{ kg/m}^3$	$\eta = 1$ $G = 7$ $J_h = 0.0552 \text{ kg.m}^2$	$P = 3; R_s = 3.3 \Omega$ $L_d = 0.0416 \text{ H}$ $L_q = 0.0416 \text{ H}$ $L_L = 0.08 \text{ H}$ $\phi_m = 0.4382 \text{ wb}$	$q_0 = 0.0061$ $q_1 = -0.0013$ $q_2 = -9.7477 * 10^{-4}$

Table III.1: Parameters of the low-power (3-kW) WECS equipped with PMSG.

II. WECS simulation results without MPPT control

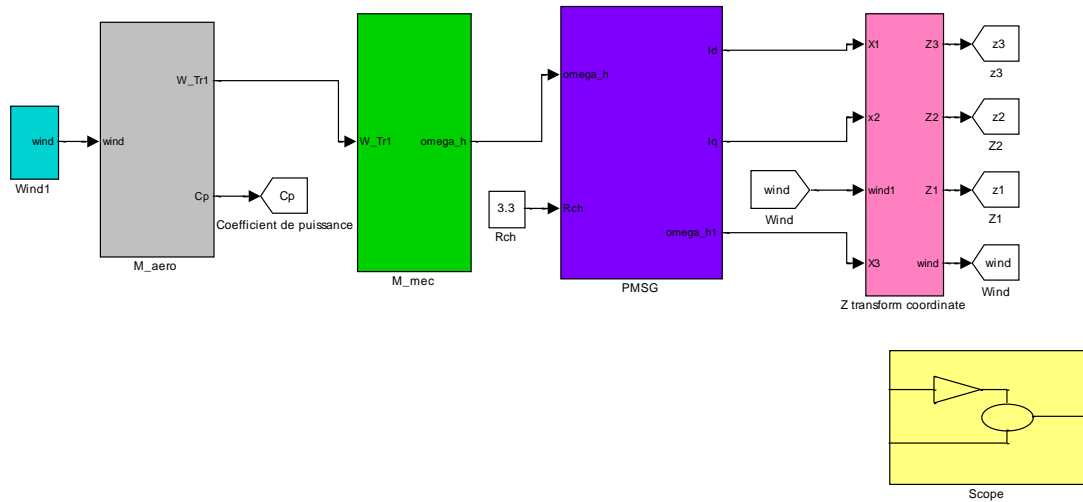


Fig. III.1: WECS Block Diagram without MPPT Control

The following Fig. III.2, shows the power coefficient without MPPT technique, where the power coefficient is between (0.1 and 1.16), while the maximum power is estimated at $C_{Pmax} = 0.467$ and the Fig. III.4 represents the mechanical power, Fig. III.3 shows the Tip speed ratio against the optimal Tip speed and we conclude that the simulation results relating to the fact that the energy efficiency of WECS is not satisfactory compared to the maximum values, so we need a MPPT control structure to ensure a good efficiency.

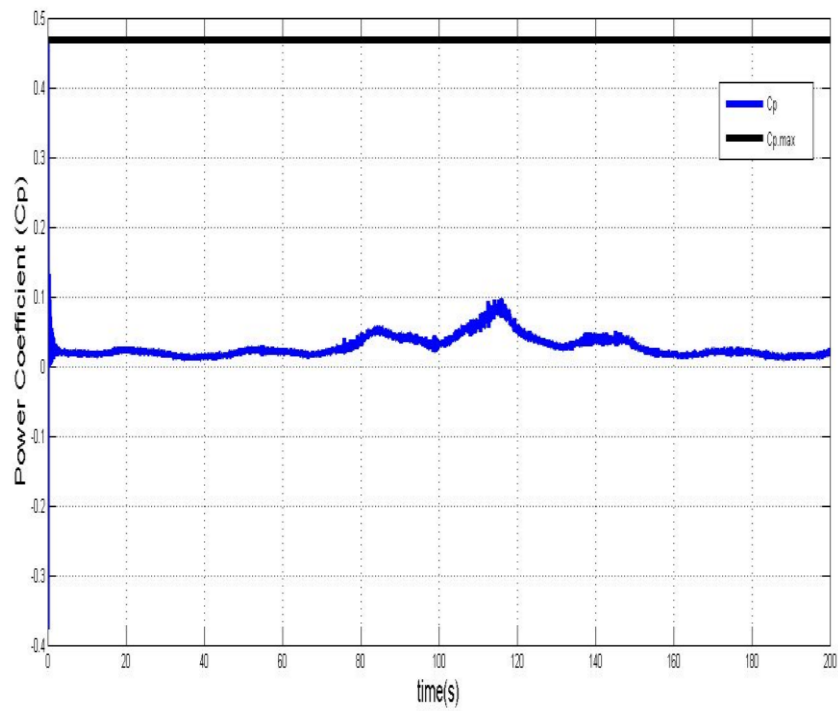


Fig. III.:2 Power Coefficient C_p .

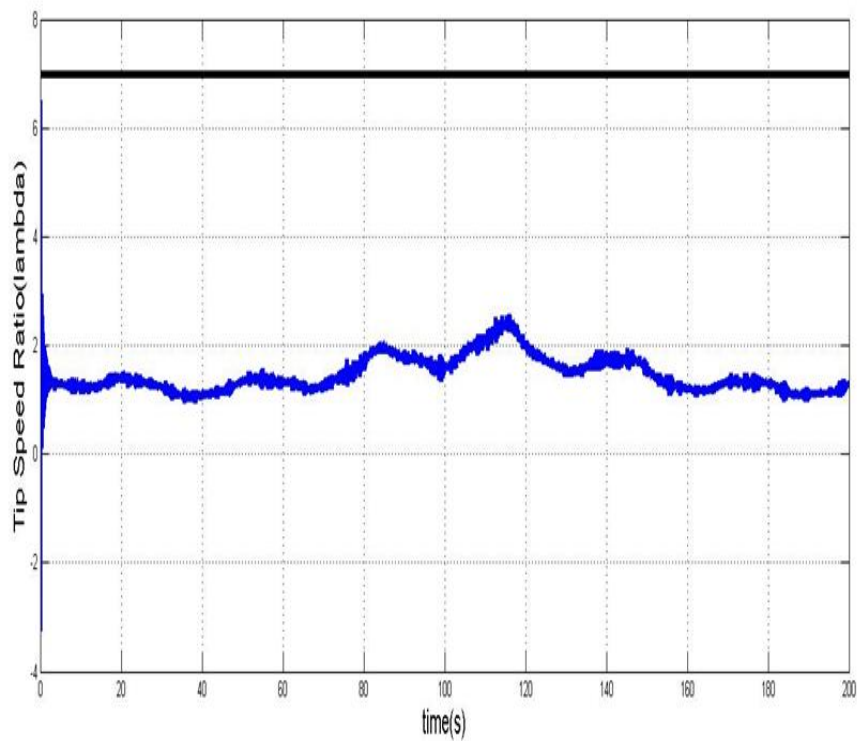


Fig. III.3: Tip speed ratio λ .

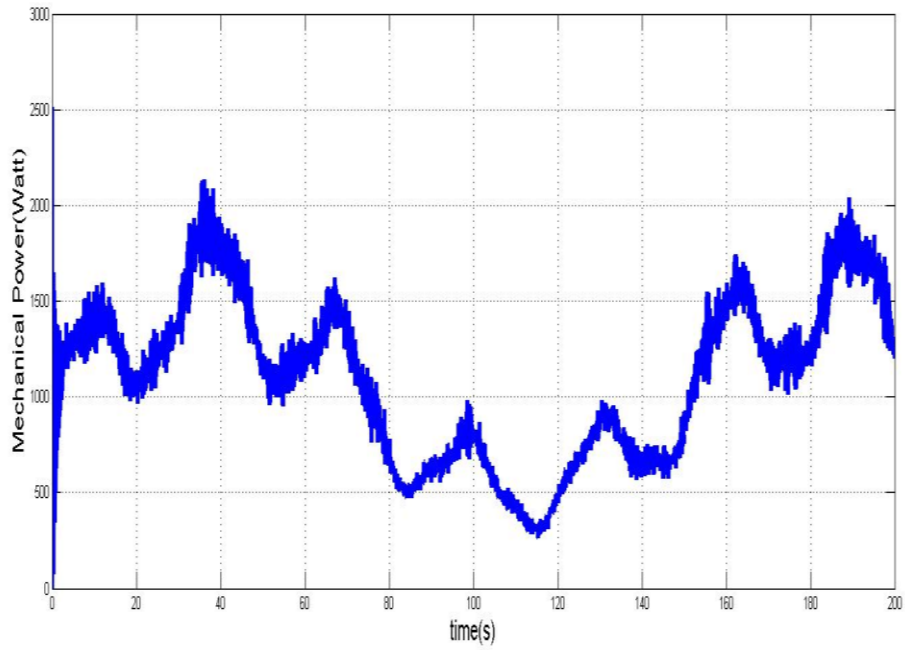


Fig.III.4: Mechanical power P_m .

III. WECS simulation results with MPPT control

In this section, we tested the robustness of two controllers for two wind profiles (Low and High Turbulence).

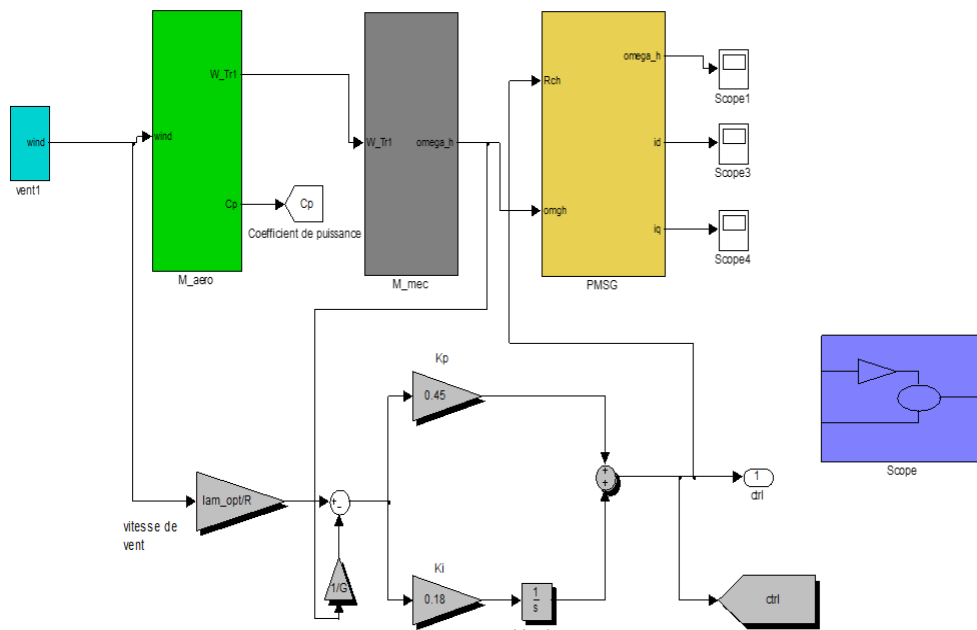


Fig.III.5: MPPT control simulation using a PI controller diagram block.

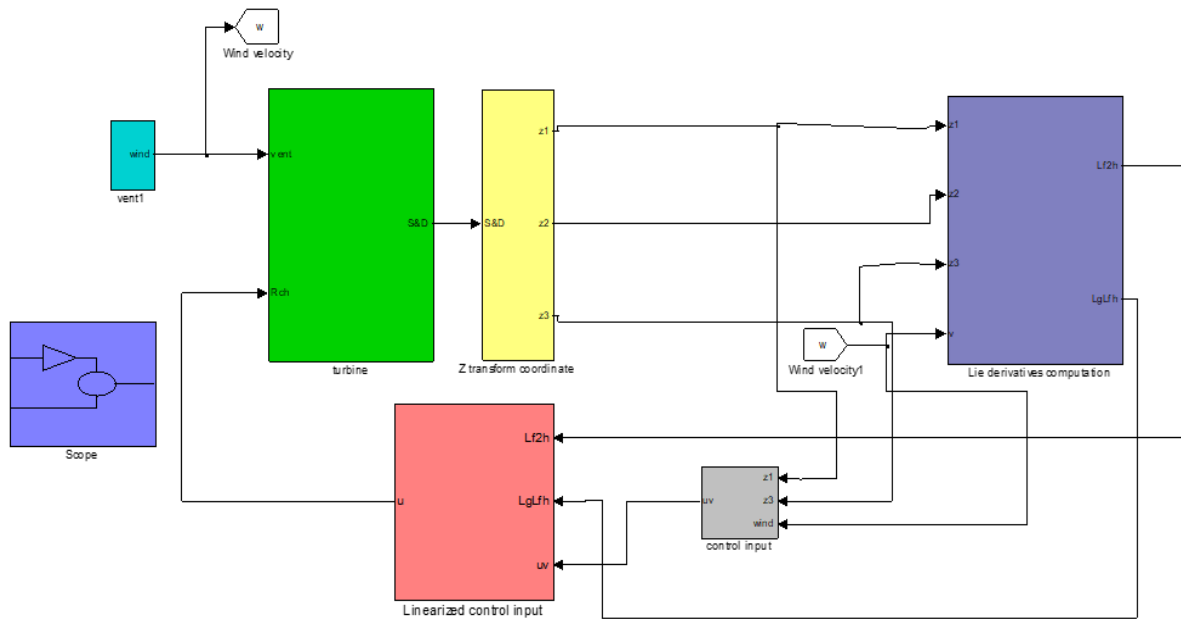


Fig.III.6: MPPT control simulation via Feedback linearization controller diagram block.

III.1. Comparative study (PI controller and FL controller)

III.1.1. Low-turbulence wind speed (DSP noise=0.001)

To verify the robustness of the system and the performance of a conventional PI speed controller, we will study the effect of a random wind speed with low disturbance varying between $V_{min}=4.5$ (m/s) and $V_{max}=10.5$ (m/s) to simulate the real variable behaviour.

In our work, the wind profile is modelled by the sum of several harmonics plus the mean of the wind speed, as follows:

$$V_m = \frac{V_{max} + V_{min}}{2} \quad \text{And} \quad v(t) = v_m + \sum_{i=1}^n A_i \sin(\omega t)$$

$$V(t) = 7.5 + 0.2 \sin(0.1047t) + 2 \sin(0.2665t) + \sin(1.2930t) + 0.2 \sin(3.6645t)$$

The Figure bellow, represents wind speed profile studied at low disturbance (Fig.III.7).

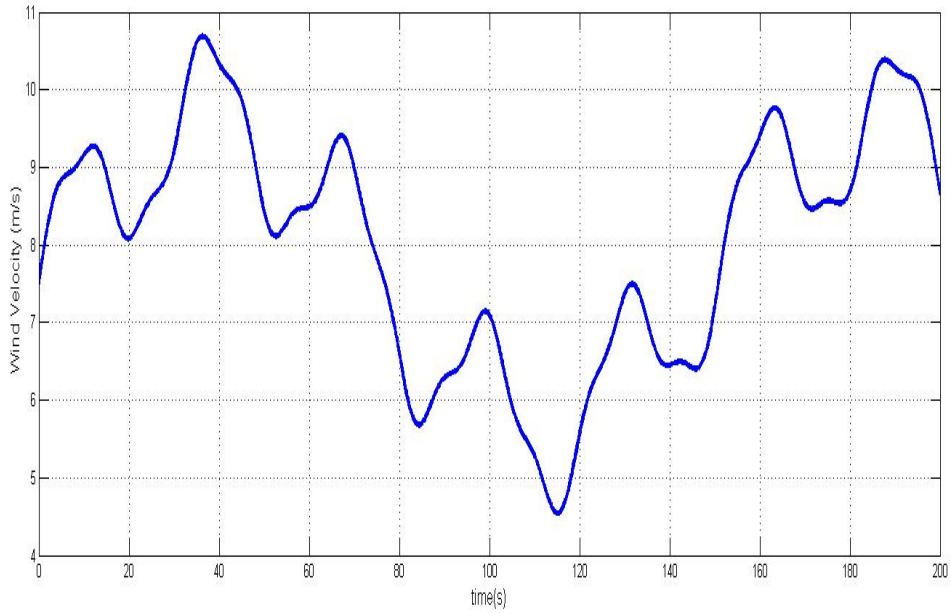


Fig. III.7: Wind speed profile with low disturbance.

The system responses are given in Fig.III.8-III.15. The test shows a satisfactory response of the wind system with low transient disturbances at the level of the power coefficient C_p (Figure.III.8), of the TSR (Figure.III.9) and of the speed of the generator (Figure.III.10). These disturbances do not influence the stability of the control structure but cause small static errors. In addition, the control performance of PI varies considerably at different wind speeds, which is due to the fact that PI control cannot maintain global control consistency.

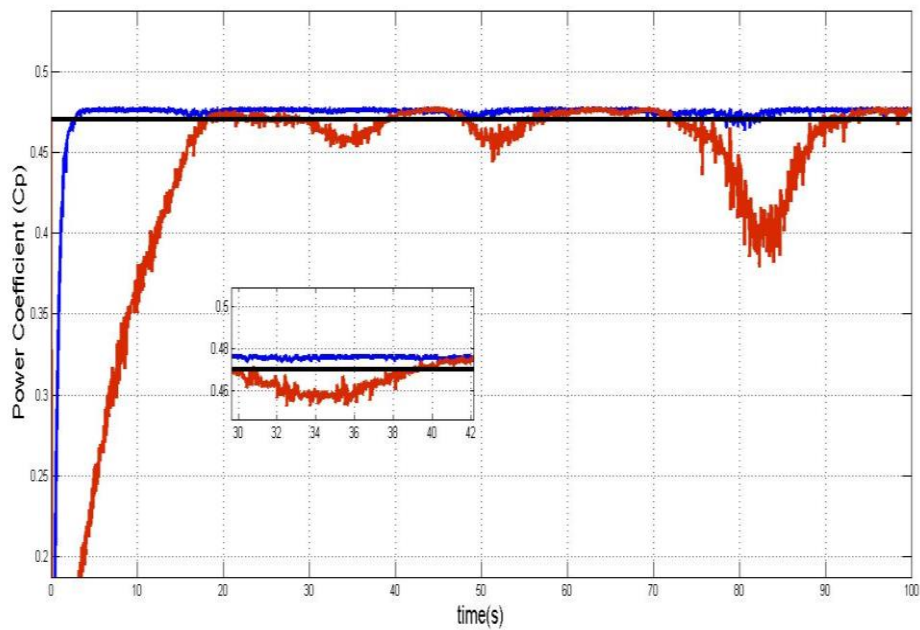


Fig.III.8: Power coefficient $C_p(t)$ for a FL controller versus a PI controller.

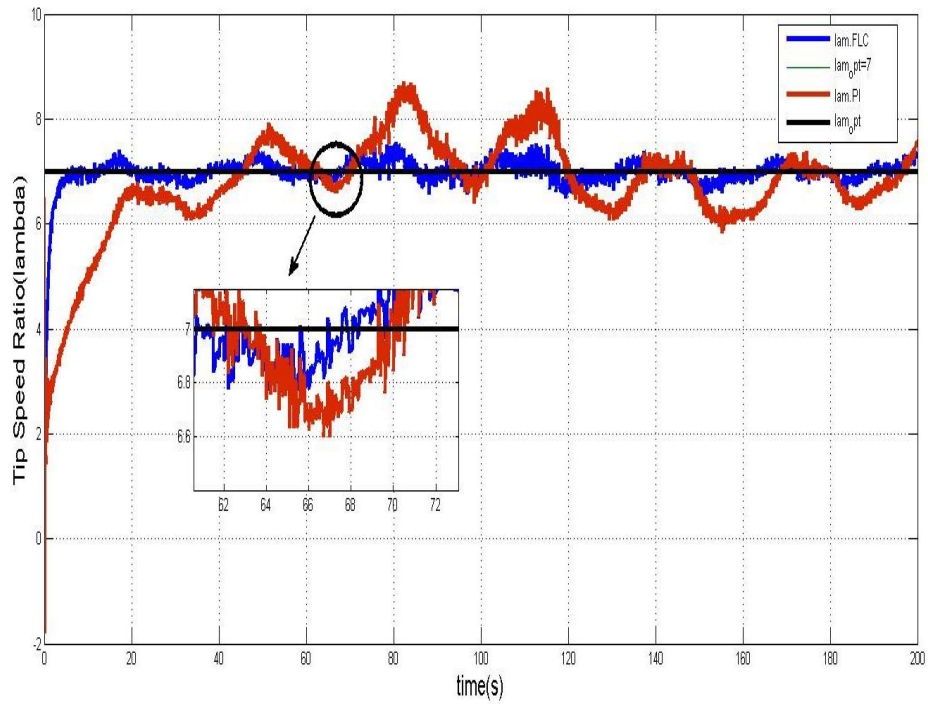


Fig.III.9: Specific speed $\lambda(t)$ for a FL controller versus a PI controller

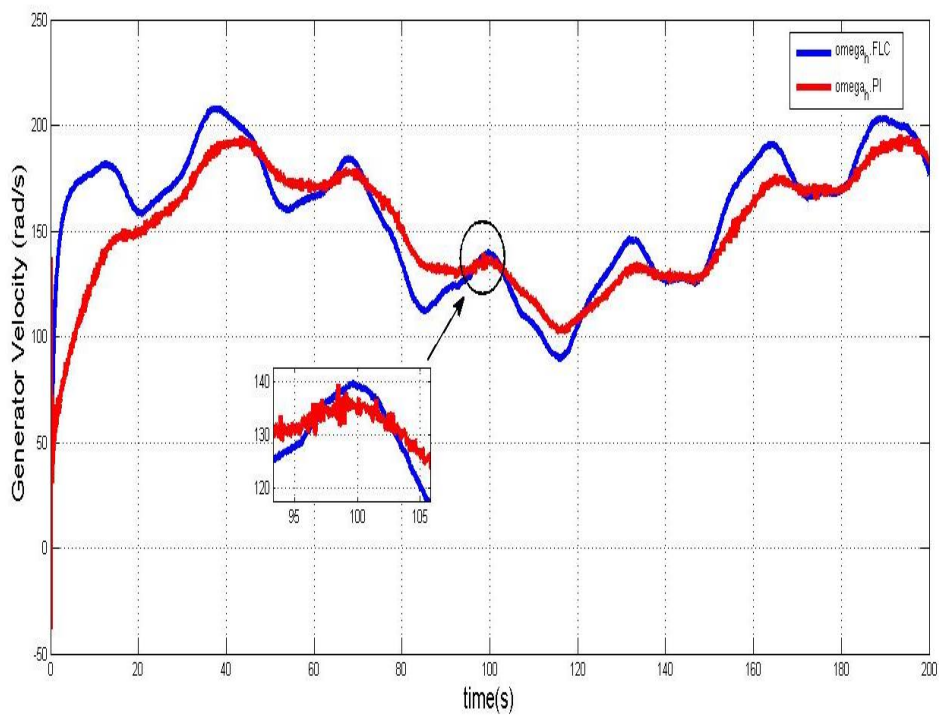


Fig.III.10: Generator speed for an FL controller versus a PI controller

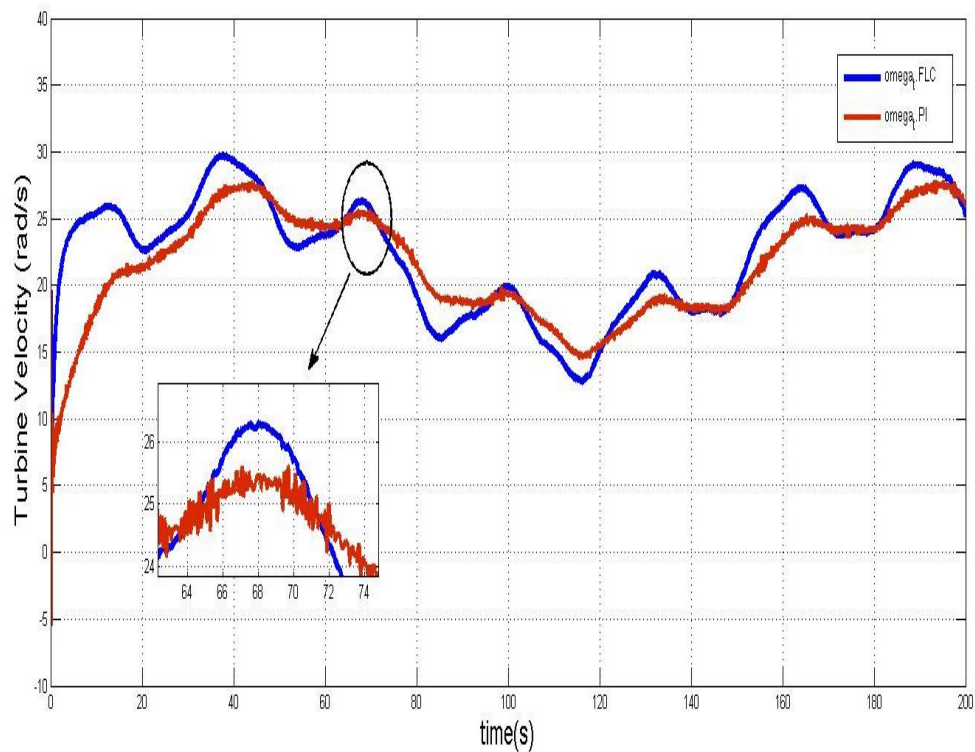


Figure III.11: Turbine speed for a FL controller versus a PI controller

In the case of low disturbance, Fig.III.11 shows that the proposed FL controller has a faster convergence than the PI controller which allows it to move closer to the baseline more quickly despite fluctuations.

Fig.III.12: compares the electromagnetic couples provided by the two controllers PI and FL respectively; we notice that after a peak at transient speed, the torque flows a value of the order of 23 N.m in steady state and stabilizes at a value of load torque.

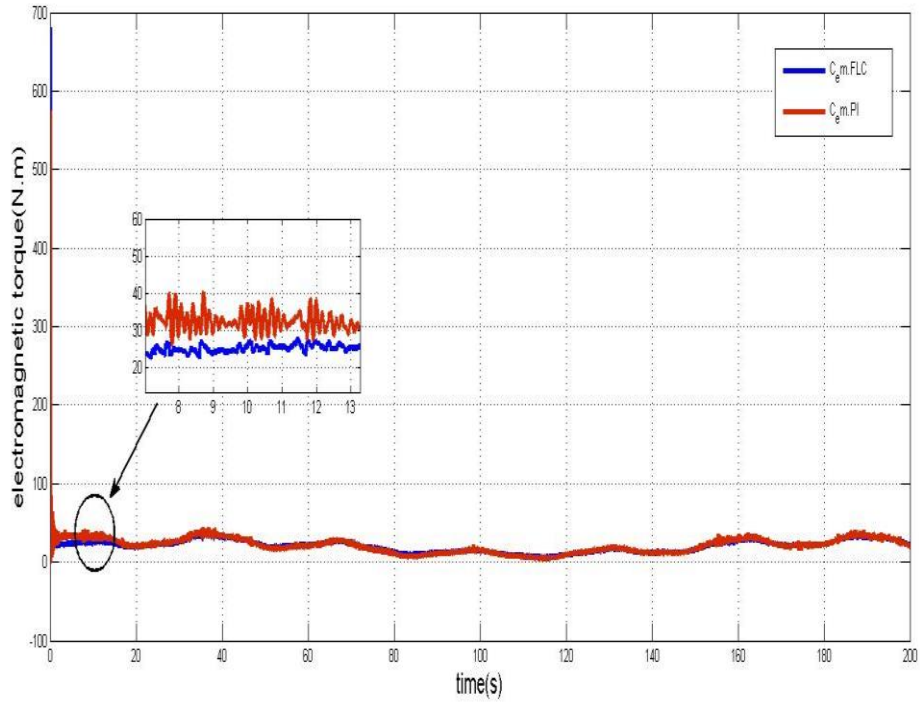


Fig.III.12: Electromagnetic torque for a FL controller versus a PI controller

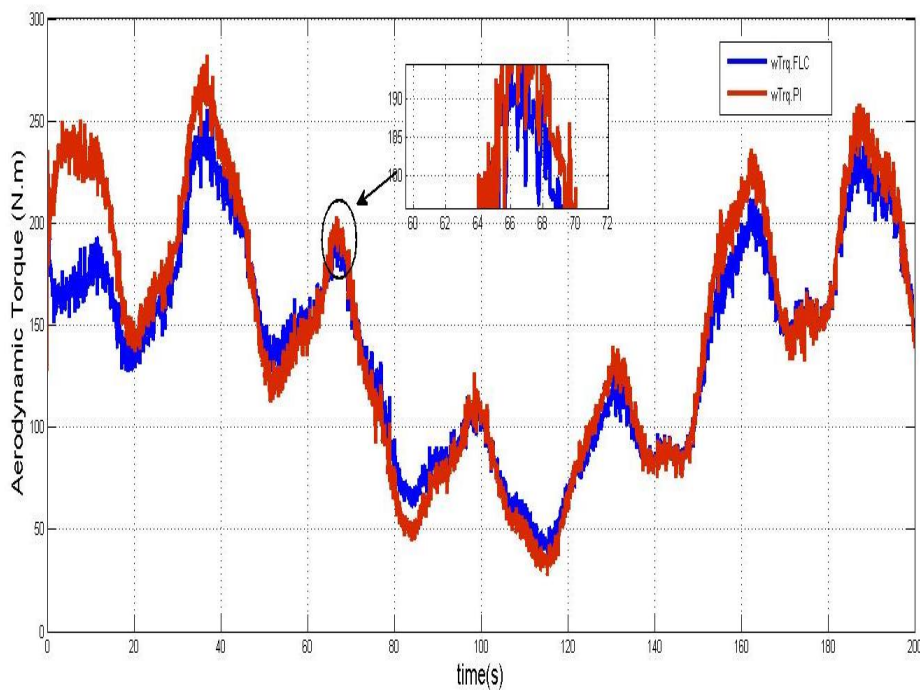


Fig.III.13: Aerodynamic torque for a FL controller versus a PI controller

The following figures represent electrical and mechanical power. It should be noted that when the wind speed increases at a specific time, the mechanical power is increased immediately.

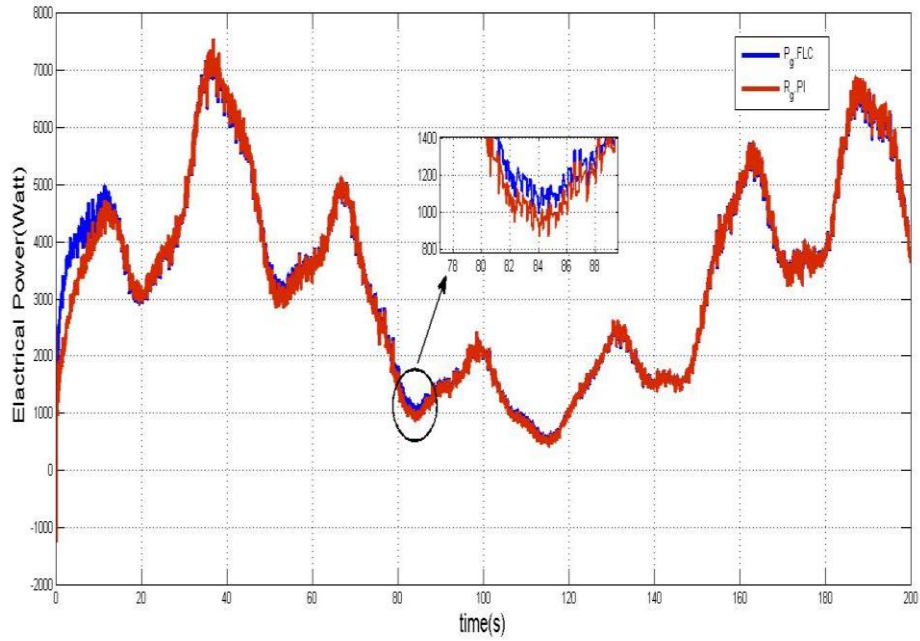


Fig.III.14: Electrical power for a FL controller versus a PI controller.

We find that the maximum of the electrical power does not generally coincide with the maximum of the mechanical power. This is due to the losses in the generator which vary from one operating point to another. We also notice that the electrical power captured by the wind turbine conversion chain is not always optimal over the entire wind speed variation range.

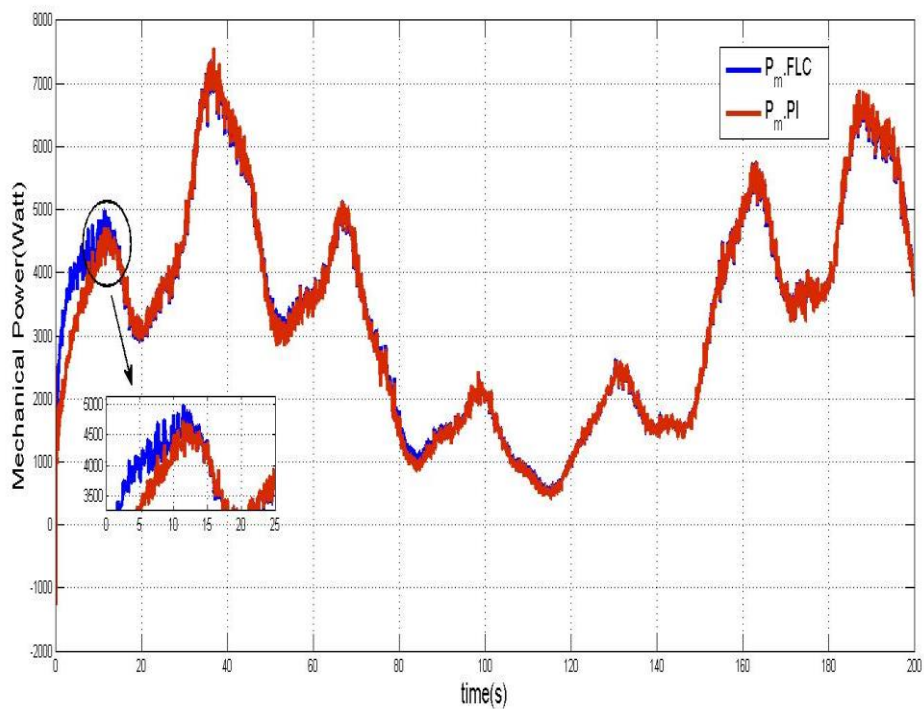


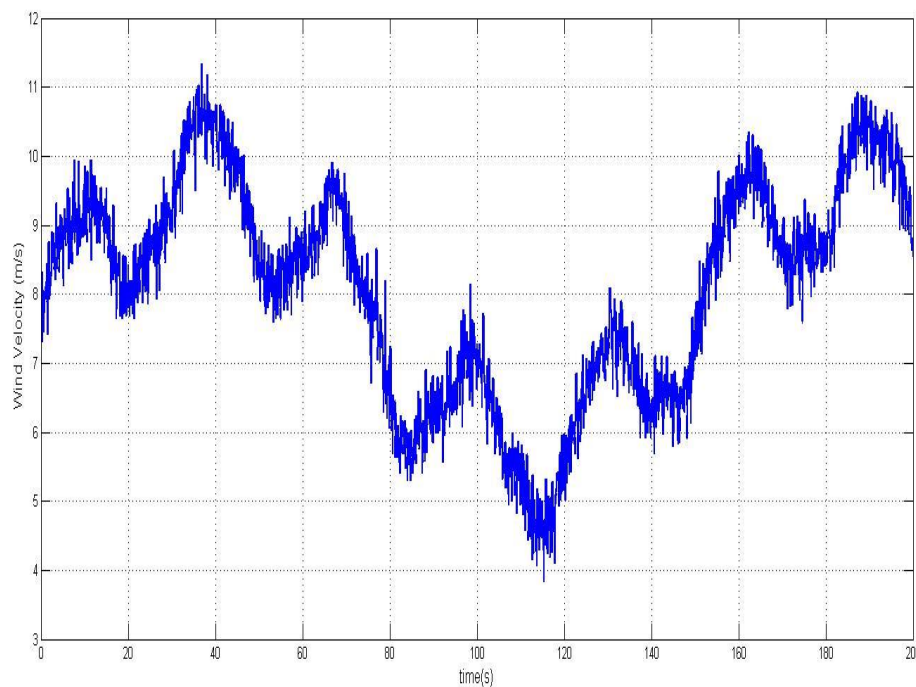
Fig.III.15: Mechanical power for a FL controller versus a PI controller**III.1.2. High-turbulence Wind speed (DSP noise= 0.01)**

To mimic strong variation in wind speed, a wind speed can change considerably, which makes MPPT a very difficult task because it requires a fast and timely response from the controller. Here a highly turbulent stochastic wind speed varying between $v_{\min}=4\text{m/s}$ and $v_{\max}=11\text{m/s}$ is tested to study the MPPT performance of each approach. the wind profil can be modeled by a sum of several harmonics plus a noise of spectral density equal to 0.01 like

$$v(t) = v_m + \sum_{i=1}^n A_i \sin(\omega t) + \text{Noise (gaussien)}$$

$$V(t) = 7.5 + 0.2 \sin(0.1047t) + 2 \sin(0.2665t) + \sin(1.2930t) + 0.2 \sin(3.6645t) + \text{white noise}$$

Fig.III.16 shows the wind speed profile studied during a high disturbance.

**Fig.III.16:** Wind speed profile with high disturbance

The simulation results obtained show the high performance of the FL control (see Fig. III.17 to III.24). We can clearly see an almost perfect tracking of the power coefficient to the maximum power coefficient curve for the FL technique (Fig.III.17). In contrast to this technique, a significant deviation from the maximum power coefficient is obtained if the PI control is applied.

The FL control allows better tracking of the generator speed (Fig.III.19), and therefore better aerodynamic efficiency (Fig.III.22) than the PI control. This is confirmed by an optimum specific speed ($\lambda=7$) (Fig.III.18) and consequently a power coefficient close to its maximum value ($C_p=0.47$).

A smooth change in C_p reduces the deviation from mechanical energy (Fig.III.24). In addition, from the point of view of power curves and aerodynamics, the FL's steering performance is also satisfactory.

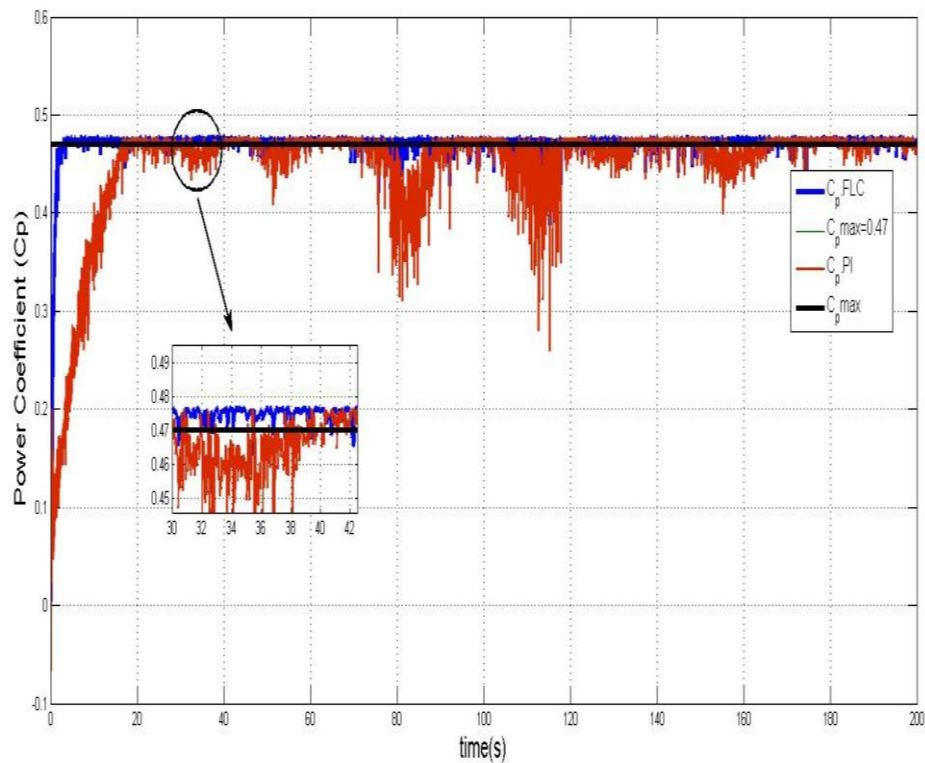


Fig.III.17: Power coefficient C_p (t) for a FL controller versus a PI controller

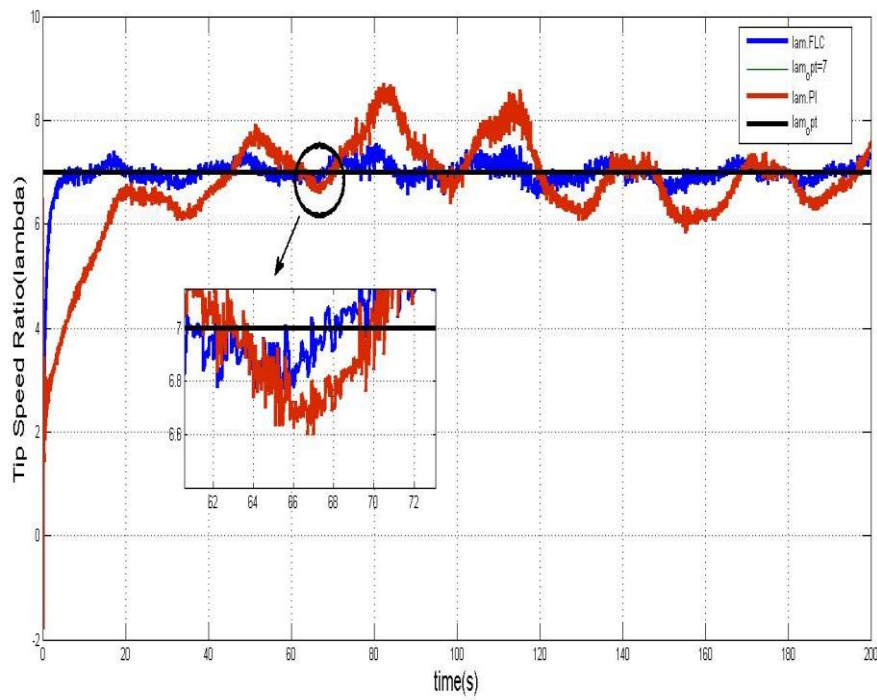


Fig.III.18: Tip speed ratio λ (t) for a FL controller versus a PI controller

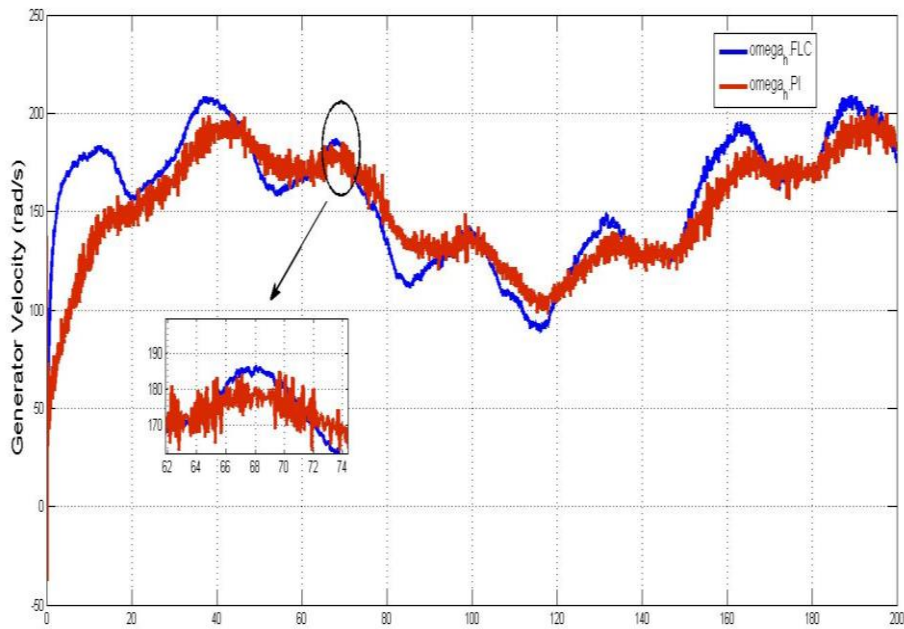


Fig.III.19: Generator speed for a FL controller versus a PI controller

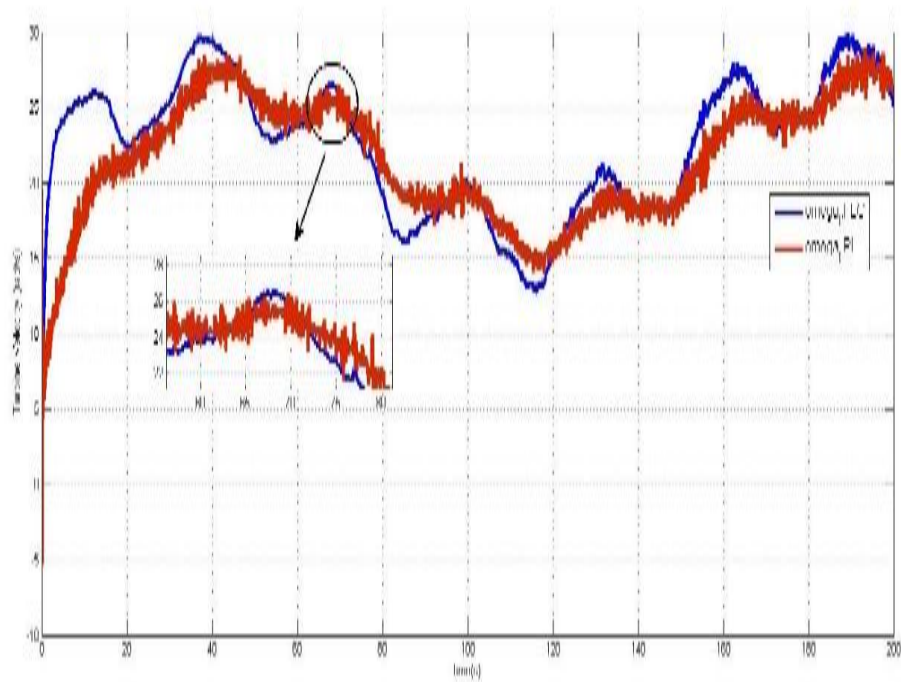


Fig.III.20: Turbine speed for a FL controller versus a PI controller

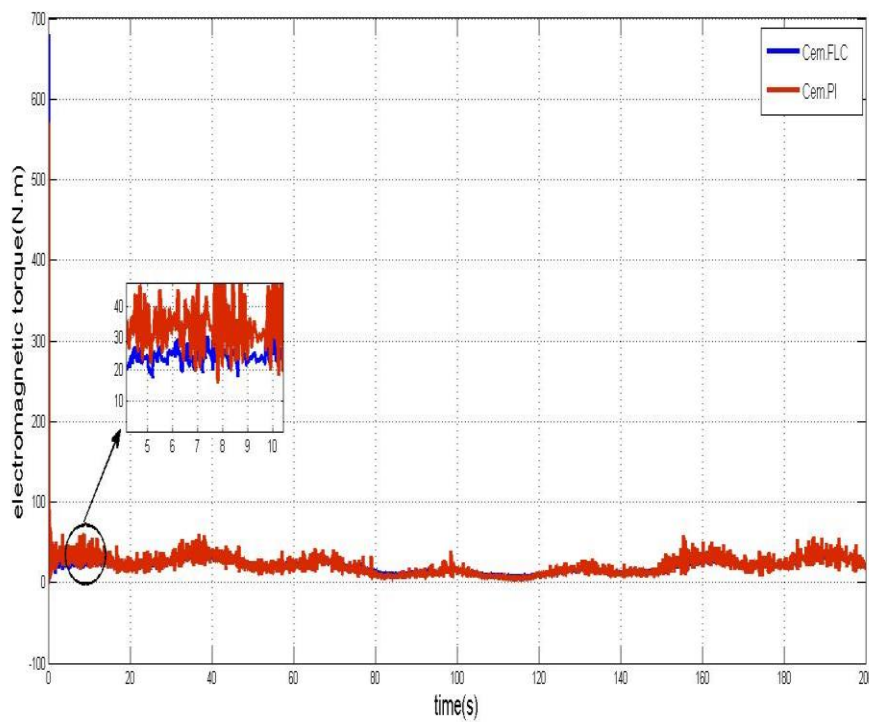


Fig.III.21: Electromagnetic torque for a FL controller versus a PI controller

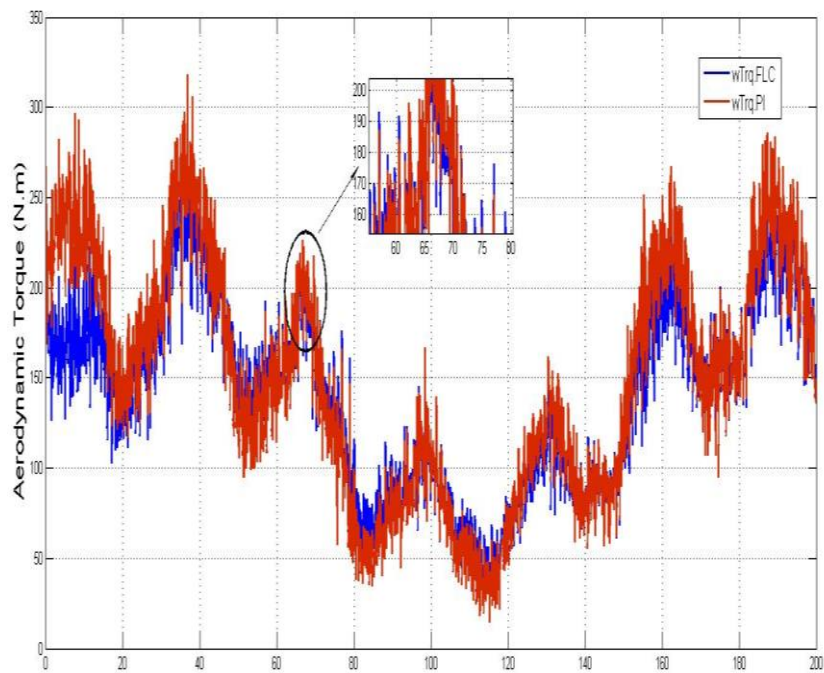


Fig.III.22: Aerodynamic torque for a FL controller versus a PI controller

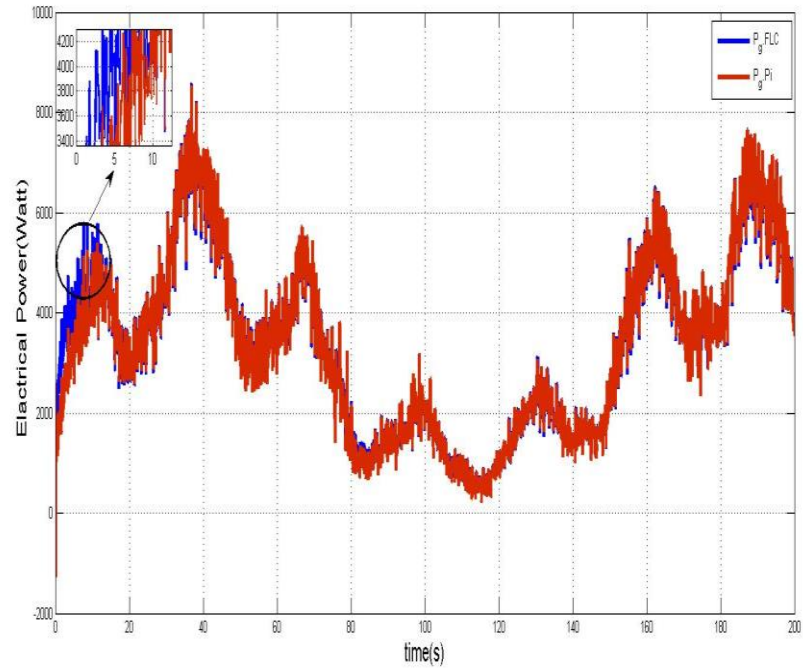


Fig.III.23: Electrical power for a FL controller versus a PI controller

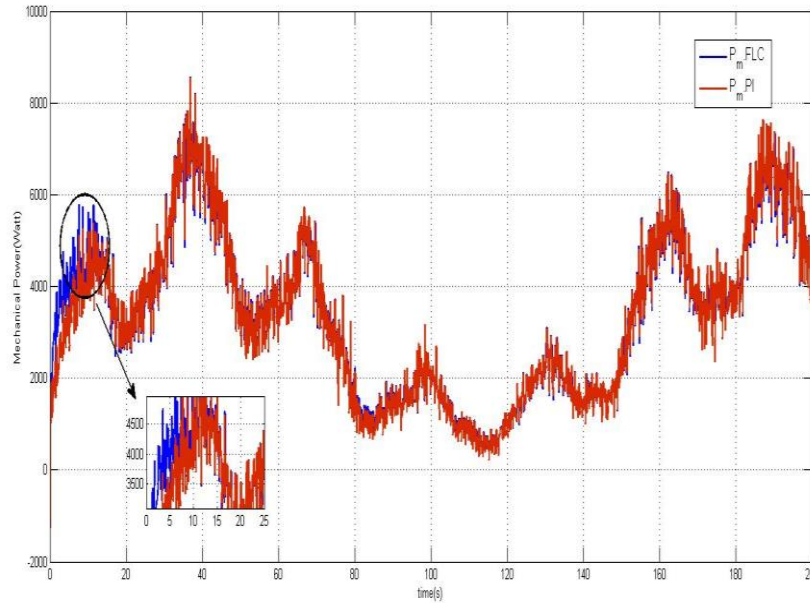


Fig.III.24: Mechanical power for a FL controller versus a PI controller

IV. Conclusion

In the last chapter, the simulation results for two wind speed profiles were used to consider the objectives set by these control strategies. Overall, the results obtained by feedback linearization control in terms of the results of the generator speed control are better than those obtained with the PI control. Especially when testing wind speed variation. We have tested FL control on WECS based PMSG in isolated process. The elaborate control treats the problems of nonlinearity of the system as well as the parametric uncertainty. It is based on the technique of feedback linearization control. The results obtained showed the performance and efficiency of the proposed control technique. In non-autonomous mode of operation or integrated into a powerful network has given good results, but it has a major drawback with regard to the dimensioning of the power converters which induces significant costs especially in the high-power ranges.



General conclusion

General conclusion

The objective of this work is the modelling of a permanent magnets synchronous generator (PMSG) with variable speeds in the case of the isolated sites, with the design of the control strategies making it possible to maximize the total output, and to control generator speed.

In order to understand the principle of operation of the wind turbine, a descriptive study of these components and these characteristics was presented in the first chapter. A state of the art was presented of the different electrical configurations used in the field of wind energy. Among the topologies cited, the choice was made on the synchronous wind turbine with permanent magnets at variable speeds. After having deduced the main aerodynamic characteristics of the turbine, the different operating zones and the control strategies used were presented. The particular area, where the maximization of the energy extracted from the wind is carried out has been detailed.

The effectiveness of the feedback linearization control has been tested on a permanent-magnet-synchronous-generator (PMSG)-based WECS in isolated operation, as detailed in Chapter 2. As analytically proven, the exact linearization is not possible in this case. A partially linearized model has thereby been obtained, in order to derive the control algorithm. The case study considered has revealed good closed-loop behaviour when the wind speed ranges from the cut-in to the rated value.

For the chapter three, the simulation results for two wind speed profiles (low and high turbulence) made it possible to consider the objectives set by these control strategies. Overall, the results obtained by the FL control in terms of generator speed regulation are better than those obtained by the PI control especially during wind speed variation tests.

This analysis could not finish without recalling that the final goal is the real world implementation of that WECS control structure most suitable for a given situation. One can remark that this choice is not necessarily a (purely technical) optimal solution, but must represent the best trade-off between closeness to the targeted optimum on the one hand and simplicity and robustness, on the other.

References

- [1] M.A HASSAD, "Influence de la commande d'une GADA des systèmes éoliens sur la stabilité des réseaux électriques", Master thesis, University Sétif 1 Alegria, 2021
- [2] Gudimindla, H., & Sandhya, S., "Performance Analysis of Adaptive Speed Reference Tracking QFT Robust Controller for Three Phase Grid connected Wind Turbine under Stochastic Wind Speed Conditions", In 2021 Emerging Trends in Industry 4.0 (ETI 4.0), pp. 1-6, 2021.
- [3] F. POITIERS, « Etude et commande de génératrices asynchrones pour l'utilisation de l'énergie éolienne-Machine asynchrone à cage autonome-Machine asynchrone à double alimentation reliée au réseau », Doctorat thesis, University of Nantes, 2003.
- [4] B. Aya, B. Bouthaina, " Contrôleur robuste d'une éolienne PMSG basé sur la technique de la rétroaction fréquentielle (Quantitative Feedback Theory QFT)", Master thesis, University Cheikh Larbi Tebessi-Tebessa, 2022
- [5] Cheikh Ridha, "Etude et Commande d'une Eolienne à base d'une Machine Synchrones à Aimants Permanents et d'une Machine Asynchrone à Double Alimentation", Doctoral thesis, University of Biskra, 2018
- [6] F. Blaabjerg, Zhe Chen, and S.B. Kjaer, "Power electronics as efficient interface in dispersed power generation systems," IEEE Trans. on Power Electronics, vol. 19, Issue: 5, pp.1184 – 1194, Sept. 2004.
- [7] Y. DJERIRI : « Commande directe du couple et des puissances d'une MADA associée à un système éolien par les techniques de l'intelligence artificielle », Thèse de doctorat université DJILLALI LIABES de sidi bel-abbés 2015.
- [8] A. B. Raju, K. Chatterjee, B. G. Fernandes « A Simple Maximum Power Point Tracker for Grid connected Variable Speed Wind Energy Conversion System with Reduced Switch Count Power Converters », 0-7803-7754-0/03/\$17.00 ©2003 IEEE
- [9] A. DAHBI : « Contribution à la Commande et à l'Amélioration des Performances de l'Énergie Électrique d'une Chaîne de Production Éolienne », Thèse de doctorat, Université Batna, 2018.
- [10] Y. DJERIRI : « Commande directe du couple et des puissances d'une MADA associée à un système éolien par les techniques de l'intelligence artificielle », Thèse de doctorat université DJILLALI LIABES de sidi bel-abbés 2015.
- [11] SAMI, KAHLA. Modélisation et commande d'un système éolien. 2018. Thèse de Doctorat. Université 8 mai 1945 de Guelma.
- [12] J.F. Manwell, J.G. McGowan, A.L. Rogers, Wind Energy Explained, Theory, Design and Application, Wiley, 2002
- [13] S. Mathew, Wind Energy Fundamentals, Resource Analysis, and Economics, Springer, 2006.
- [14] O. Guerri, "L'Énergie Eolienne en Algérie : un Bref Aperçu", Bulletin des Energies Renouvelables N°. 21, CDER, Ministère de l'Enseignement Supérieur et la Recherche Scientifique, Algeria, 2011.
- [15] H. Jeong, K. Lee, S. Choi, W. Choi, "Performance improvement of LCL-filter-based gridconnected inverters using PQR power transformation". IEEE Transactions on Power Electronics, 2010, vol. 25, no. 5, pp. 1320-1330. doi: <https://doi.org/10.1109/tpel.2009.2037225>.
- [16] A. MIRECKI « Etude comparative de chaînes de conversion d'énergie dédiées à

- une éolienne de petite puissance » Doctoral thesis, INPT de France, 2005.
- [17] Dalala, Z. M., Zahid, Z. U., & Lai, J. S., "New overall control strategy for small-scale WECS in MPPT and stall regions with mode transfer control", IEEE transactions on energy conversion, 28(4), 1082-1092, 2013.
- [18] F. Poitier, 'Etude et commande de génératrice asynchrone pour l'utilisation de l'énergie éolienne – Machine asynchrone à cage autonome – Machine asynchrone à double alimentation reliée au réseau ', Doctoral thesis d'Etat en Electronique et Génie Electrique, Ecole Polytechnique of University of Nantes, 2003.
- [19] L. Louze, "Production décentralisée de l'énergie électrique : modélisation et contrôle d'une génératrice asynchrone auto excitée", Doctoral thesis, University of Mentouri –Constantine, 2010.
- [20] L. Y. Pao and K. E. Johnson, "Control of wind turbines," IEEE Control System magazine, vol. 31, no. 2, pp. 44-62, 2011.
- [21] Affaf Rabhi, "Modélisation et présentation d'un générateur synchrone à aimant permanent dédiée à la production de l'énergie éolienne", Master thesis, University Adrar, 2019.
- [22] M. Mohamed. Toufik et Naili Abdelhadi, "Contrôle et optimisation d'une chaîne éolienne raccordée au réseau électrique à base d'un générateur synchrone à aimants permanents", Master thesis in Energy Renewable en Électrotechnique, University of Msila, 2019.
- [23] Guy Cunty « Eoliennes et aérogénérateurs, guide de l'énergie éolienne », Edissud, Aix-en-Provence, 2001
- [24] M. LOPEZ, « contribution à l'optimisation d'un système de conversion éolien pour une unité de production isolée » ; Doctoral thesis, University of Paris-Sud 11, France, 2007.
- [25] HAMECHA Samira, Ep. BOUREKACHE, "Etude et Commande d'une Eolienne à base d'une Machine Synchrone à Aimants Permanents," Magister thesis, University of Tizi-Ouzou, 2013.
- [26] D. Fernando. H. Battista, R. Mantz; 'Wind Turbine Control Systems 'Edition Springer' 2007.
- [27] M. LOPEZ, « contribution à l'optimisation d'un système de conversion éolien pour une unité de production isolée » ; Doctoral thesis, University de Paris-Sud 11, France, 2007.
- [28] Dr. Gary L. Johnson « Wind Energy Systems », Chapter 4-Wind Turbine Power, Nov, 2001
- [29] P. Leconte, M. Rapin, E. Széchenyi, « Éoliennes », Techniques de l'Ingénieur, BM 4 640.
- [30] H. Ben Ahmed, « Généralités sur l'énergie éolienne et convertisseurs associés et convertisseurs associés », séminaire électrotechnique de l'académie de Rennes, 9 mars 2004.
- [31] D.Fatou, " Étude d'une chaîne de conversion d'énergie éolienne A base de machine synchrone à aimants permanents", MASTER thesis, University Badji-Mokhtar of Annaba, 2018
- [32] J. W. Chapman et al, " Stabilizing a multi machine power system via decentralized feedback, linearizing excitation control", IEEE Transactions on Power Systems, vol. 8, no. 3, pp. 830-838, 1993
- [33] P. Leconte, M. Rapin, E. Szechenyi, << Eolienne >>, Techniques de l'Ingénieur, BM

4640

- [34] Mayouf Messaoud « la modélisation de l'aérogénérateur synchrone à aimant permanent », Magister thesis, University of Batna, 13-02-2008.
- [35] A.E. Fitzgerald, C. Kingsley, Jr., and S.D. Umans; "*Electric Machinery*", Textbook *Sixth Edition*. New York: McGraw-Hill, 2003
- [36] Chaîne de conversion éolienne de petite puissance à axe horizontal », Magister thesis ; University Badji Mokhtar-Annaba, 2009
- [37] B. Yang, T. Yu, H.C. Shu, et al, " Passivity based sliding mode control design for optimal power extraction of a PMSG based variable speed wind turbine, «Renew Energy. 2018; 119:577-589
- [38] *Chettout Abdelhak, Brachouche Yacine* « Etude et maximisation d'un système éolienne à base d'une machine synchrone à aimants permanents », Master thesis, 2018
- [39] R. Cheikh et al, "Robust nonlinear control via feedback linearization and Lyapunov theory for Permanent magnet synchronous generator-based wind energy conversion system", *Front. Energy, (Springer), No. 46, Vol. 12, pp 1–12, 2018.*
- [40] Mousa, H. H., Youssef, A. R., & Mohamed, E. E.," Adaptive P&O MPPT algorithm-based wind generation system using realistic wind fluctuations", *International Journal of Electrical Power & Energy Systems, 112, 294-308, 2019.*